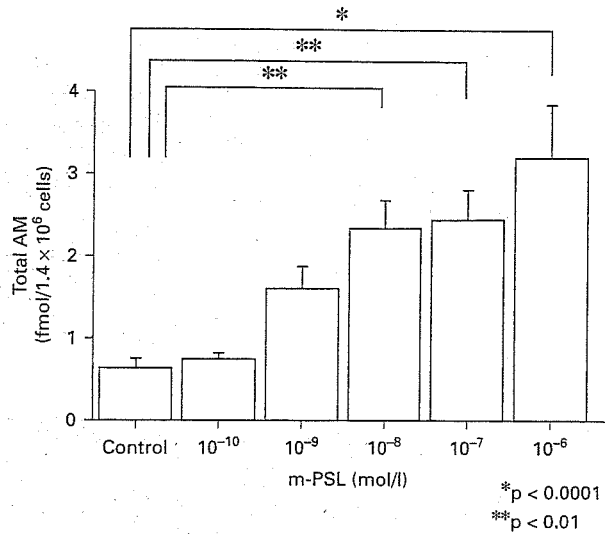

2

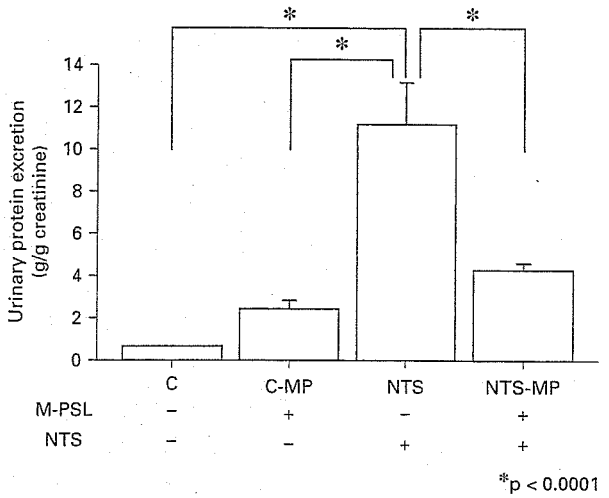

4

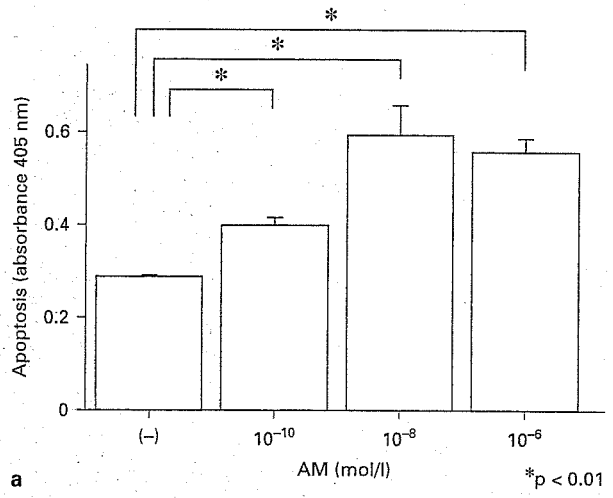

a

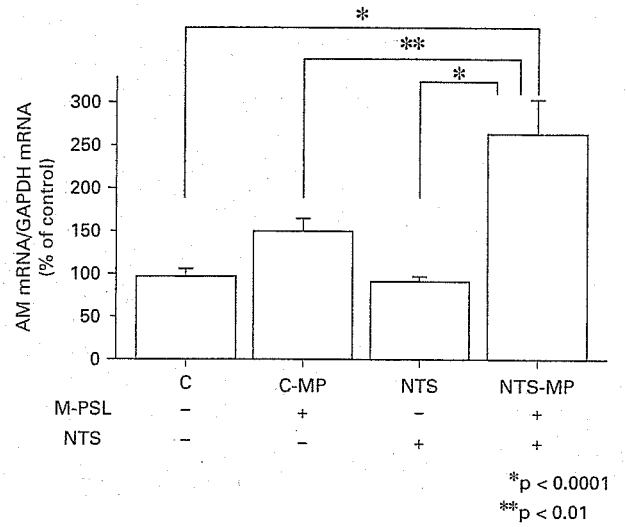

5

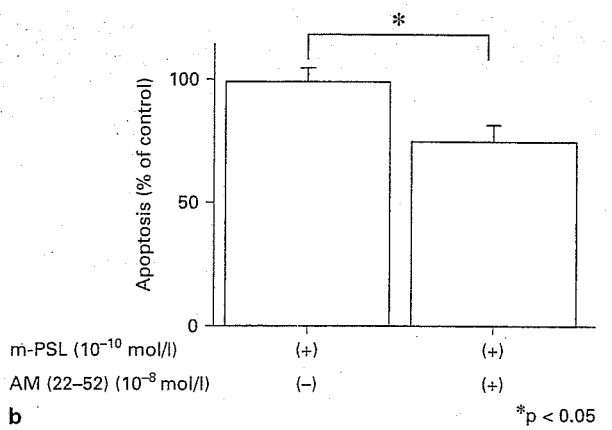

b

3

Fig. 2. Changes of adrenomedullin secretion from the rat cultural mesangial cells by methylprednisolone treatment. Values are expressed as the mean ± SEM (n = 6). * $p < 0.0001$, ** $p < 0.01$.

Fig. 3. a Changes of mesangial cell apoptosis by adrenomedullin treatment. Values are expressed as the mean ± SEM (n = 3). * $p < 0.01$, compared to control cells. **b** Effect of adrenomedullin receptor antagonist AM(22-52) on the apoptosis of rat mesangial cells. Values are expressed as the mean ± SEM (n = 4). * $p < 0.05$

Fig. 4. Urinary protein excretion in the control (C), control treated with methylprednisolone (C-MP), anti-GBM glomerulonephritis model (NTS) and NTS rat groups treated with methylprednisolone (NTS-MP). Values are expressed as the mean ± SEM (n = 6). * $p < 0.0001$.

Fig. 5. Glomerular adrenomedullin expression in the control (C), control treated with methylprednisolone (C-MP), anti-GBM glomerulonephritis model (NTS) and NTS rat groups treated with methylprednisolone (NTS-MP). Values are expressed as the mean ± SEM (n = 6). * $p < 0.0001$, ** $p < 0.01$.

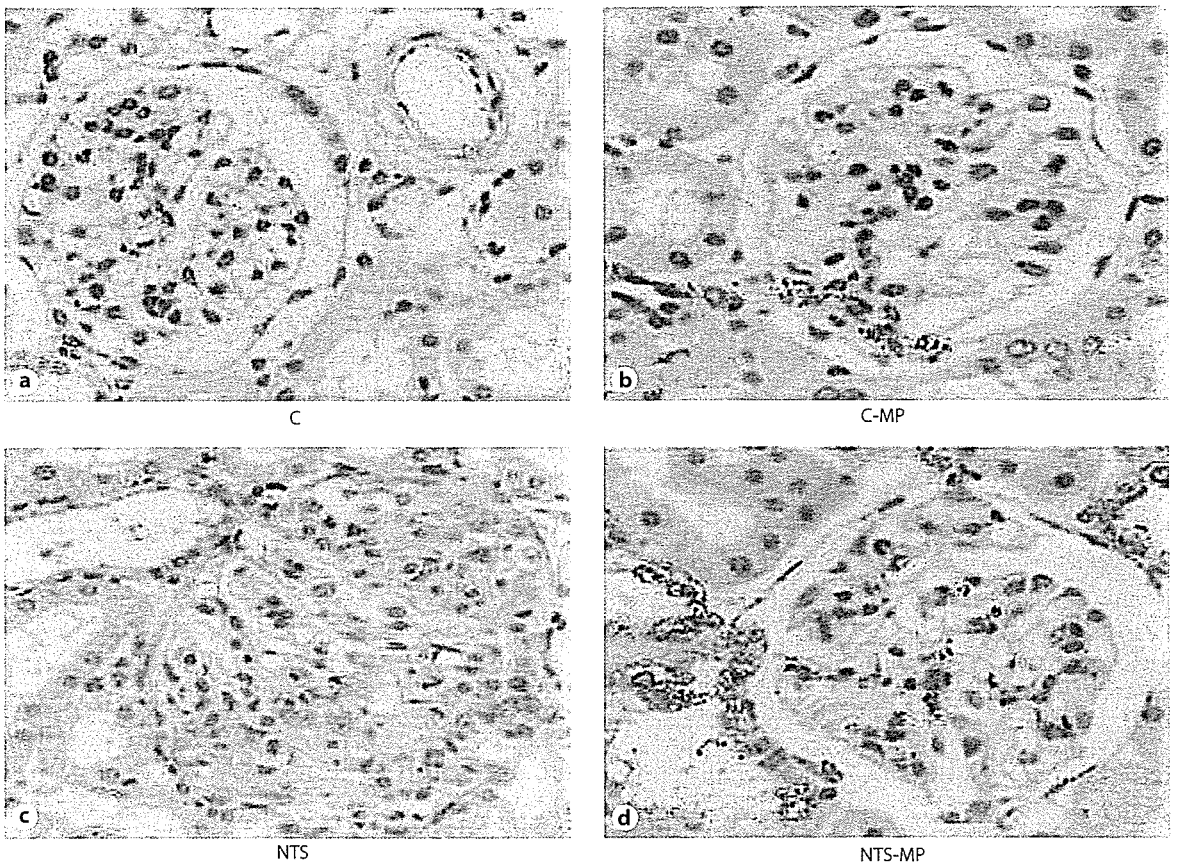

Fig. 6. Immunohistochemical staining of adrenomedullin (browny spot) in rat kidneys from the control (C), control treated with methylprednisolone (C-MP), anti-GBM glomerulonephritis model (NTS), and NTS rat groups treated with methylprednisolone (NTS-MP).

of 10^{-8} *M* AM(22-52) into the cultured MCs compared to the control (m-PSL plus AM(22-52) vs. m-PSL alone, 76 vs. 100%, $p < 0.05$, respectively) (fig. 3b).

Effect of m-PSL on NTS Rats

Urinary protein excretion was remarkably increased in NTS rats, while its level was significantly lower in NTS-MP rats than in NTS rats (fig. 4). Histologically, MCs proliferation and crescent formation were reduced in NTS-MP rats (fig. 1c). In immunofluorescence staining, m-PSL did not affect the rabbit IgG deposition in glomeruli, but reduced the glomerular deposition of rat IgG in NTS-MP rats.

AM Expression and Immunohistochemistry

Glomerular AM expressions were not different among groups C, C-MP and NTS. On the other hand, the AM mRNA levels were significantly increased in NTS-MP rats compared to NTS or C-MP rats (NTS-MP rats vs. control rats, C-MP rats, NTS rats, 270 vs. 100, 153, 94%, $p < 0.0001$, $p < 0.01$, $p < 0.0001$, respectively) (fig. 5). In immunohistochemistry, AM staining was obscure in group C, C-MP and NTS (fig. 6a–c). On the other hand, in the NTS-MP rats, AM was significantly increased in the mesangial area (fig. 6d). The area staining positive for AM, determined by a color imaging morphometric analysis system, was significantly increased in NTS-MP rats compared with the control, C-MP or NTS rats (NTS-MP rats vs. control rats, C-MP rats, NTS rats, 1.85 vs. 0.18, 0.34, 0.54%, $p < 0.0001$) (fig. 7).

Discussion

In studies using cultured cells, such as vascular wall cells, fibroblasts and macrophages, AM secretion was found to be generally stimulated by inflammatory cytokines, lipopolysaccharide and hormones [20, 25]. The se-

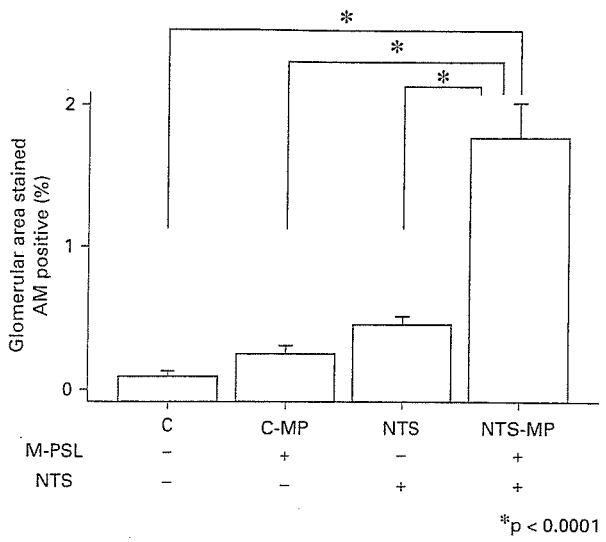

Fig. 7. Glomerular adrenomedullin production evaluated in the control (C), control treated with methylprednisolone (C-MP), anti-GBM glomerulonephritis model (NTS) and NTS rat groups treated with methylprednisolone (NTS-MP). Values are expressed as the mean ± SEM (20 glomeruli per kidney section). * $p < 0.0001$.

cretion of AM was also increased in the cultured endothelial cells, vascular smooth muscle cells, and cardiac fibroblasts by treatment with glucocorticoid, while it was suppressed in macrophages by that of dexamethasone [19, 20, 25]. Our study showed that treatment with m-PSL induced an increase in AM secretion from cultured rat MCs in a concentration-dependent manner. AM inhibited the MCs proliferation stimulated by PDGF in a concentration-dependent manner, as previously reported [4, 6–10]. In addition, it was confirmed that AM increased the MCs apoptosis, while AM(22-52) inhibited the MCs apoptosis, as in a previous study [12]. Based on these findings obtained from the culture studies, we next examined the relationships among the regulation of AM, renal histological lesions and the treatment of m-PSL in the rat model of GN.

We started the treatment with m-PSL for anti-GBM GN rats on day 3, when MCs had slightly proliferated m-PSL therapy inhibited the subsequent MCs proliferation, crescent formation and proteinuria associated with the increased expression and production of AM in glomeruli. Considering the present culture studies, these findings suggest that the glomerular AM increased by m-PSL therapy might inhibit the MCs proliferation and the progression of anti-GBM GN, while it might induce the MCs apoptosis and the resolution of anti-GBM GN. Some reports show the favorable actions of AM on renal damage [13–18], but there are few in vivo studies investigating the role of glomerular AM in GN. Recently, Plank et al. [18] showed that exogenous AM injection reduces the MC number in the state of MC proliferation in a model of mesangioproliferative GN. This report is consistent with our present study in the point that AM plays renoprotective roles in GN, partly via the inhibition of MC proliferation. M-PSL administration, at a dose of more than 10^{-8} *M*, induced the increase in AM secretion from the cultured rat MCs, but m-PSL treatment did not upregulate the expression of glomerular AM in the control rats in our in vivo study. The discrepancy may be caused by the differences in m-PSL concentrations and other circumstances in local areas. On the other hand, m-PSL treatment upregulated the expression and production of glomerular AM in NTS rats. The different state of mesangial cells, such as steady or recovery phases, may be related to these results.

There are also human studies suggesting the relationships between AM in the kidney and renal disease. The urinary excretion of AM, probably derived from the kidney, but not from the blood stream, is negatively correlated with urinary protein excretion and the severity of glomerular lesions [26–28]. Immunohistochemical studies performed by Kuo et al. [29] show that the glomerular production of AM is decreased in IgA nephropathy patients without impaired renal function. Similar to our present study, these findings indicate a protective role of AM against mesangial proliferative glomerular damage. The progression of glomerular disease is characterized by MCs proliferation, and then the accumulation of mesangial extracellular matrix. MC apoptosis has been proposed to be an important mechanism of resolution in mesangial proliferative GN [11]. Glucocorticoid therapy sometimes improves these glomerular lesions, and ameliorates clinical abnormalities. Considering the increased production of AM in MCs following m-PSL treatment, and the antiproliferative and apoptotic effects of AM on MCs, the renoprotective effect of glucocorticoids on GN might occur partly through the AM produced by MCs. Further studies, including experimentation of AM administration of anti-GBM GN rats, will be necessary to determine the role of AM in the improvement of anti-GBM GN.

References

1 Kitamura K, Kangawa K, Kwamoto M, Ichiki Y, Nakamura S, Matsuo H, Eto T: Adrenomedullin: a novel hypotensive peptide isolated from human pheochromocytoma. Biochem Biophys Res Commun 1993;192:553–560.

2 Eto T, Kato J, Kitamura K: Regulation of production and secretion of adrenomedullin in the cardiovascular system. Regul Pept 2003;112: 61–69.

3 Jougasaki M, Wei CM, Aarhus LL, Heublein DM, Sandberg SM, Burnett JC: Renal localization and actions of adrenomedullin: a natriuretic peptide. Am J Physiol Renal Physiol 1995;268:F657–F663.

4 Chini EN, Chini CCS, Bolliger C, Jougasaki M, Grande JP, Burnett JC, Dousa TP: Cytoprotective effects of adrenomedullin in glomerular cell injury: central role of cAMP signaling pathway. Kidney Int 1997;52:917–925.

5 Hino M, Nagase M, Kaname S, Shibata S, Nagase T, Oba S, Funaki M, Kobayashi N, Kawachi H, Mundel P, Fujita T: Expression and regulation of adrenomedullin in renal glomerular podocytes. Biochem Biophys Res Commun 2005;330:178–185.

6 Parameswaran N, Nambi P, Brooks DP, Spielman WS: Regulation of glomerular mesangial cell proliferation in culture by adrenomedullin. Eur J Pharmacol 1999;372:85–95.

7 Chini EN, Choi E, Grande JP, Burnett JC, Dousa TP: Adrenomedullin suppresses mitogenesis in rat mesangial cells via cAMP pathway. Biochem Biophys Res Commum 1995; 215:868–873.

8 Michibata H, Mukoyama M, Tanaka I, Suga S, Nakagawa M, Ishibashi R, Goto M, Akaji K, Fujiwara Y, Kiso Y, Nakao K: Autocrine/paracrine role of adrenomedullin in cultured endothelial and mesangial cells. Kidney Int 1998; 53:979–985.

9 Segawa K, Minami K, Sata T, Kuroiwa A, Shigematsu A: Inhibitory effect of adrenomedullin on rat mesangial cell mitogenesis. Nephron 1996;74:577–579.

10 Osajima A, Kato H, Uezono Y, Suda T, Okazaki M, Oishi Y, Tamura M, Tanaka H, Izumi F, Nakashima Y: Adrenomedullin inhibits transmural pressure induced mesangial cell proliferation through activation of protein kinase A. Nephron 1999;83:352–357.

11 Baker AJ, Mooney A, Hughes J, Lombardi D, Johnson RJ, Savill J: Mesangial cell apoptosis: the major mechanism for resolution of glomerular hypercellularity in experimental mesangial proliferative nephritis. J. Clin. Invest 1994;94:2105–2116.

12 Parameswaran N, Nambi P, Brooks DP, Spielman WS: Regulation of glomerular mesangial cell proliferation in culture by adrenomedullin. Eur J Pharmacol 1999;372:85–95.

13 Nishikimi T, Mori Y, Kobayashi N, Tadokoro K, Wang X, Akimoto K, Yoshihara F, Kangawa K, Matsuoka H: Renoprotective effect of chronic adrenomedullin infusion in Dahl salt-sensitive rats. Hypertension 2002;39:1077–1082.

14 Nagae T, Mukoyama M, Sugawara A, Mori K, Yahata K, Kasahara M, Suganami T, Makino H, Fujinaga Y, Yoshioka T, Tanaka I, Nakao K: Rat receptor-activity-modifying proteins (RAMPs) for adrenomedullin/CGRP receptor: cloning and upreguration in obstructive nephropathy. Biochem Biophys Res Commun 2000;270:89–93.

15 Nishimatsu H, Hirata Y, Shindo T, Kurihara H, Kakoki M, Nagata D, Hayakawa H, Satonaka H, Sata M, Tojo A, Suzuki E, Kangawa K, Matsuo H, Kitamura T, Nagai R: Role of endogenous adrenomedullin in the regulation of vascular tone and ischemic renal injury. Circ Res 2002;90:657–663.

16 Dobrzynski E, Montanari D, Agata J, Zhu J, Chao J, Chao L: Adrenomedullin improves cardiac function and prevents renal damage in streptozotocin-induced diabetic rats. Am J Physiol Endocrinol Metab 2002;283:E1291–E1298.

17 Matsumoto M, Fujimoto S, Iwatsubo S, Sato Y, Hara S, Kitamura K, Eto T: Adrenomedullin (AM) and receptor- activity-modifying proteins in glomeruli with thy.1 glomerulonephritis. Clin Exp Nephrol 2004;8:316–321.

18 Plank C, Hartner A, Klanke B, Geissler B, Porst M, Amann K, Hilgers KF, Rascher W, Dotsch J: Adrenomedullin reduces mesangial cell number and glomerular inflammation in experimental mesangioproliferative glomerulonephritis. Kidney Int 2005;68:1086–1095.

19 Ishihara T, Kato J, Kitamura K, Katoh F, Fujimoto S, Kangawa K, Eto T: Production of adrenomedullin in human vascular endothelial cells. Life Sci 1997;60:1763–1769.

20 Tomoda Y, Isumi Y, Katafuchi T, Minamino N: Regulation of adrenomedullin secretion from cultured cells. Peptides 2001;22:1783–1794.

21 Yamaga J, Hashida S, Kitamura K, Tokashiki M, Aoki T, Inatsu H, Ishikawa N, Kangawa K, Morishita K, Eto T: Direct measurement of glycine-extended adrenomedullin in plasma and tissue using an ultrasensitive immune complex transfer enzyme immunoassay in rats. Hypertens Res 2003;26(suppl):S45–S53.

22 Kanno K, Okumura F, Toriumi W, Ishiyama N, Nishiyama S, Naito K: Nephrotoxic serum-induced nephritis in Wistar-Kyoto rats: a model to evaluate antinephritic agents. Jpn J Pharmacol 1998;77:129–135.

23 Ou ZL, Nakayama K, Natori Y, Doi N, Saito T, Natori Y: Effective methylprednisolone dose in experimental crescentic glomerulonephritis. Am J Kidney Dis 2001;37:411–417.

24 Ohta H, Tsuji T, Asai S, Sasakura K, Teraoka H, Kitamura K, Kangawa K: One-step direct assay for mature-type adrenomedullin with monoclonal antibodies. Clin Chem 1999;45: 244–251.

25 Kubo A, Minamino K, Isumi Y, Katafuchi T, Kangawa K, Dohi K, Matsuo H: Production of adrenomedullin in macrophage cell line and peritoneal macrophage. J Biol Chem 1998;273: 16730–16738.

26 Kubo A, Iwano M, Minamino N, Sato H, Nishino T, Hirata E, Akai Y, Shiiki H, Kitamura K, Kangawa K, Matsuo H, Dohi K: Measurement of plasma and urinary adrenomedullin in patients with IgA nephropathy. Nephron 1998;78:389–394.

27 Kubo A, Kurioka H, Minamino N, Nishitani Y, Sato H, Nishino T, Iwano M, Shiiki H, Kangawa K, Matsuo H, Dohi K: Plasma and urinary levels of adrenomedullin in chronic glomerulonephritis patients with proteinuria. Nephron 1998;80:227–230.

28 Eto T, Kitamura K: Adrenomedullin and its role in renal diseases. Nephron 2001;89:121–134.

29 Kuo MC, Kuo HT, Chiu YW, Chang JM, Guh JY, Lai YH, Chen HC: Decreased synthesis of glomerular adrenomedullin in patients with IgA nephropathy. J Lab Clin Med 2005;145: 233–238.

Original Article

Long-Term Anti-Hypertensive Therapy with Benidipine Improves Arterial Stiffness over Blood Pressure Lowering

Toshihiro KITA, Yoshihiko SUZUKI, Tanenao ETO, and Kazuo KITAMURA

Pulse wave velocity (PWV) reflects arterial stiffness and is an independent predictor of cardiovascular mortality and morbidity. However, because it is closely related to blood pressure (BP), PWV is an imperfect measure for evaluating the effects of anti-hypertensive drugs on arterial wall properties. To clarify the effect of benidipine on arterial properties, we first derived the regression line between BP and PWV changes in a short-term experiment. Using this line, we evaluated the long-term effect of benidipine on PWV changes. In the short-term experiment, 29 participants were intravenously administered nicardipine for 90 min. Maximum decreases of brachial-ankle PWV (baPWV) were plotted against the corresponding decreases in BP. In the long-term experiment, 9 hypertensive patients were treated with benidipine for 1 year, during which BP and baPWV were monitored. After 1 year, benidipine was suspended for 2 weeks, and BP and baPWV were reevaluated. In the short-term experiment, PWV was dependent on BP only, and the equation of the regression line was ΔPWV (cm/s) $=10.114 \times \Delta$MBP (mmHg) ($r=0.913$) or ΔPWV (%) $=0.719 \times \Delta$MBP (%) ($r=0.926$). In the long-term therapy, benidipine treatment achieved stable BP control within 3 months; the real PWV decreases (r-PWV) were almost identical to the PWV decrease estimated (e-PWV) from BP lowering at 3 months. However, r-PWV exceeded e-PWV after 6 months. Relative BP and PWV improvements compared to the control were maintained 2 weeks after suspension of benidipine. In conclusion, long-term benidipine administration improves arterial wall properties beyond what can be accounted for by changes in BP. (*Hypertens Res* 2005; 28: 959–964)

Key Words: **pulse wave velocity, blood pressure, benidipine, nicardipine, human**

Introduction

Arterial stiffness has been recognized as an important indicator of increased cardiovascular risk. Several studies have clearly demonstrated that increased arterial stiffness, as determined by pulse wave velocity (PWV), is a strong risk factor for cardiovascular morbidity and mortality (*1–3*). PWV measurement has been rapidly deployed in medical practice since a convenient automated pulse wave analyzer became available commercially in Japan. Brachial-ankle PWV (baPWV) derived using the automated analyzer is also closely related to risk factors and/or the organ damage characteristic of cardiovascular diseases (*4–9*). Moreover, significant improvements in baPWV have been observed after anti-hypertensive treatments with different classes of drugs (*10–12*), and thus

From the First Department of Internal Medicine, Miyazaki Medical College, University of Miyazaki, Miyazaki.

This study was supporoted in part by Grants-in-Aid for Scientific Research and for the 21st Century Centers of Excellence Program (Life Sciences) from the Ministry of Education, Culture, Sports, Science and Technology, Japan, and for the Program for Strategic Regional Science and Technology Advancement.

Address for Reprints: Toshihiro Kita, M.D., Ph.D., First Department of Internal Medicine, Miyazaki Medical College, University of Miyazaki, 5200 Kihara, Kiyotake, Miyazaki 889–1692, Japan. E-mail: t-kita@po.sphere.ne.jp

Received July 11, 2005; Accepted in revised form October 17, 2005.

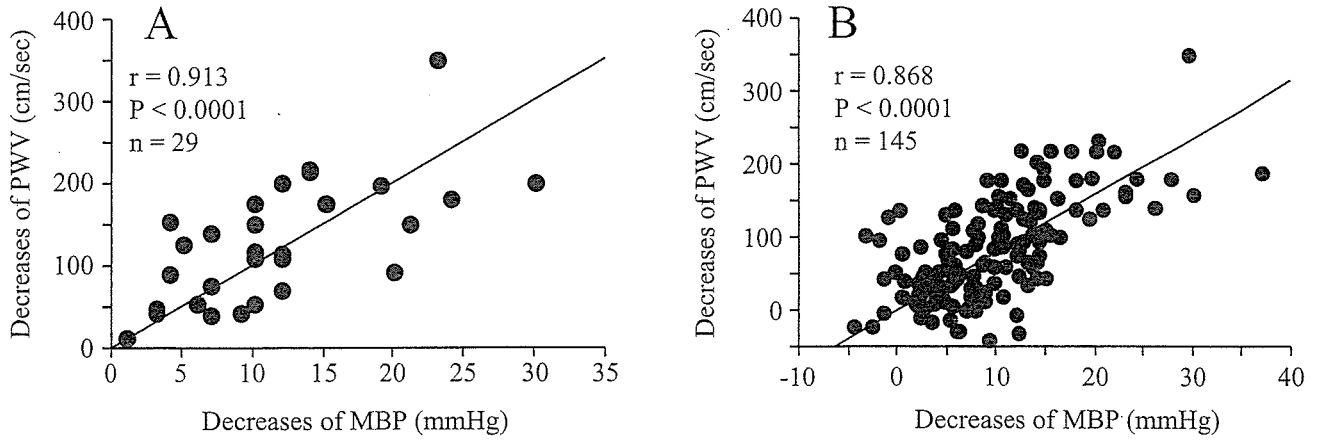

Fig. 1. *A: The correlation between maximum changes of mean blood pressure (MBP) and concomitant changes of pulse wave velocity (PWV) after nicardipine administration. B: The correlation between the changes of MBP and PWV in all-data analysis.*

Table 1. Time-Dependent Effects of Benidipine on the Indicated Parameters

	Control	Treatment with benidipine			2 week after suspension
		6 months	12 months	*p* in trend	
SBP (mmHg)	158.8±3.6	127.1±3.3**	128.8±3.0**	<0.0001	146.0±4.5##
DBP (mmHg)	96.7±4.0	80.6±3.1**	79.9±3.2**	0.0012	87.7±4.0##
MBP (mmHg)	117.4±3.4	96.1±2.9**	96.2±2.2**	<0.0001	107.1±4.4##
HR (bpm)†	69.1±2.7	69.3±3.2	69.1±3.4	1.00	63.8±1.6
PWV (cm/s)	1,768±100	1,464±59*	1,449±69**	0.012	1,631±77#
CRP (ng/ml)	1,163±279	651±108	520±101*	0.05	716±232
t-AM (fmol/ml)	12.8±0.8	12.2±0.3	12.5±0.4	0.78	14.0±0.7
m-AM (fmol/ml)	1.68±0.16	1.66±0.15	1.59±0.10	0.90	1.75±0.23
ET-1 (pg/ml)	2.04±0.16	1.79±0.19	1.84±0.17	0.57	1.56±0.11
PRA (ng/ml/h)	1.06±0.20	1.84±0.23	1.69±0.35	0.11	0.86±0.14
PAC (pg/ml)	92.7±9.1	104.8±9.8	100.4±10.6	0.68	103.4±14.0
IRI (μU/ml)	13.7±6.1	11.9±6.0	8.8±1.8	0.79	9.4±3.3

SBP, systolic blood pressure; DBP, diastolic blood pressure; MBP, mean blood pressure; HR, heart rate; PWV, pulse wave velocity; CRP, C-reactive protein; t-AM, total adrenomedullin; m-AM, mature adrenomedullin; ET-1, endothelin-1; PRA, plasma renin activity; PAC, plasma aldosterone concentration; IRI, immunoreactive insulin. *$p<0.05$, **$p<0.01$, compared to control (ANOVA); #$p<0.05$, ##$p<0.01$, compared to control (paired *t*-test). †HR was measured by ECG.

baPWV may be a surrogate marker of the efficacy of anti-hypertensive therapy. However, baPWV, like authentic PWV, is itself closely dependent on blood pressure (BP); thus it has been difficult to evaluate whether improvements in baPWV with anti-hypertensive therapy really reflect an improvement in arterial properties.

Ca^{2+} channel blockers (CAB) have been reported to possess anti-sclerotic properties, and CAB have improved cervical artery and coronary artery sclerosis in randomized controlled trials (*13–15*). Benidipine has additional beneficial actions on endothelial function and inhibits intimal thickening in animal studies (*16–18*); thus benidipine could be a more effective treatment for arterial sclerosis in hypertensive patients. To clarify the effect of benidipine on arterial properties, we first derived the regression line between BP and baPWV changes in a short-term experiment using nicardipine. We then used this regression line to evaluate the long-term effect of benidipine on baPWV changes separately from BP changes in hypertensive patients.

Methods

Short-Term Experiment

Participants

Twenty-nine male participants, mean age 46.0±9.2 years, were enrolled in this study. All participants received screening examinations including urine and blood tests, ECG, chest

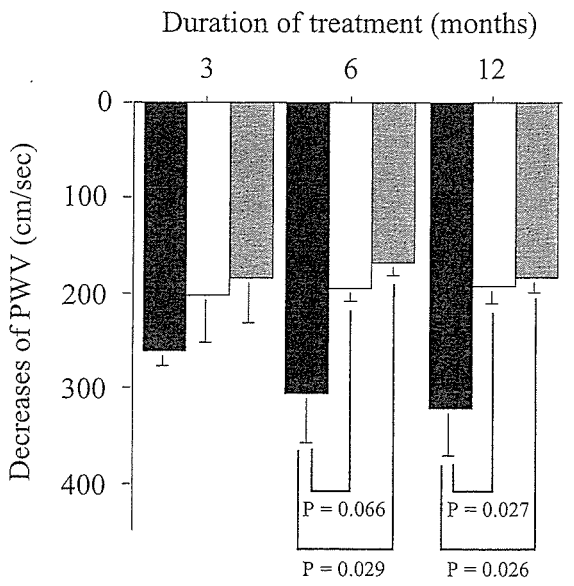

Fig. 2. *Comparison between real pulse wave velocity (PWV) changes (closed column) and estimated PWV changes (open column: analysis with maximum changes; gray column: all-data analysis) after benidipine treatment in hypertensive patients (mean±SEM, n=9). Estimated PWV changes were calculated from blood pressure changes as described in the text.*

X-ray, and echocardiography. They were diagnosed as normotensive (n=11), hypertensive (n=11), or diabetic (n=8), and one patient had both hypertension and diabetes mellitus. They were not receiving any medication, nor was there any evidence of heart failure (left ventricular ejection fraction <50%), renal failure (serum creatinine >1.0 mg/dl), peripheral artery disease, or a history of cardiovascular accidents. The study was approved by the ethics committee of our institute, and all participants gave written informed consent.

Study Protocol

All experiments were started at 9 AM in the fasting state. One 20-gauge cannula was inserted into the forearm vein for infusion of 0.9% saline. Saline was infused at a rate of 100 ml/h throughout the experiments. Baseline measurements were obtained after a 60 min equilibration period. Nicardipine (1 μg/min/kg) was then administered intravenously for 90 min, followed by a 90 min saline only infusion. After 45 min, the dosage of nicardipine was increased to 1.5 μg/min/kg to generate a 10% reduction of systolic BP (SBP), but was not increased above 1.5 μg/min/kg for safety reasons, even when a small BP reduction occurred. For convenience, BP was monitored every 10 min using an automated hemodynamometer with a brachial cuff. At 15 min intervals, PWV, BP and heart rate were measured using an automatic waveform analyzer (form PWV/ABI, BP-203RPE; Colin Medical Technology Co., Komaki, Japan) as reported previously (*4*). Maximum reductions in PWV were observed at 60–90 min after nicardipine infusion. Maximum reductions in PWV and concomitant BP reductions were plotted (linear regression), and the regression formula obtained. All data obtained during nicardipine infusion (5 points per person) were also analyzed by multivariate regression analysis.

Long-Term Treatment

Patients

Twelve patients with untreated essential hypertension were enrolled in this study. However, two patients dropped out within 3 months and one patient had uncontrollable hypertension. The remaining nine patients (53.0±13.3 years of age, 6 men and 3 women) completed the study and were used for the analysis. All patients received screening examinations, including urine and blood tests, ECG, chest X-ray, and echocardiography. No patient was receiving medication for hypertension, and no patient had heart failure, renal failure, peripheral artery disease, or a history of cardiovascular accidents. Three patients had hypercholesterolemia (total cholesterol >240 mg/dl), but no patient had diabetes mellitus. The study was approved by the ethics committee of our institute, and all patients gave written informed consent.

Protocol

Nine patients were treated with benidipine 4 to 8 mg/day only and all patients achieved BP <140/90 mmHg within 3 months. BP and pulse rate were measured in our outpatients office every month, and PWV was monitored at 0, 3, 6, and 12 months with an automatic waveform analyzer. After completion of 1-year of treatment, benidipine was suspended for 2 weeks in all patients with informed consent. BP and PWV were reevaluated after suspension. Not only PWV, but also BP and heart rate were measured by an automatic waveform analyzer for all data analyses.

Blood samples were taken at 0, 6, and 12 months and used to measure biochemical parameters and vasoactive factors. High-sensitivity C-reactive protein (hsCRP) was measured by latex nephelometry (Dade Behring, Marburg, Germany). Plasma concentration of adrenomedullin was measured with an immunoradiometric assay kit (AM RIA Shionogi, Osaka, Japan), and endothelin-1 levels were measured using a commercially available standard radioimmunoassay kit.

Statistical Analyses

All statistical analyses were performed using StatView-J software (version 4.5; Abacus Concepts, Inc., Berkeley, USA) on a Macintosh computer. After confirmation of normal distributions for all variables, the significance of differences was evaluated by paired t-test or analysis of variance (ANOVA) followed by Fisher's multiple comparison tests. Relationships between variables were analyzed by simple correlation analysis and multivariate regression analysis. Data are expressed as

the mean±SEM and a p value <0.05 was the criterion for statistical significance.

Results

Short-Term Experiment

Nicardipine administration achieved a 10.2±1.3% decrease in SBP and an 11.9±1.3% decrease in diastolic BP (DBP) accompanied by an 8.7±0.8% decrease in PWV and a 13.2±1.5% increase in heart rate. BP and PWV quickly recovered after termination of nicardipine treatment. Maximum decreases in PWV and concomitant BP changes were plotted by linear regression analysis. The changes of SBP and DBP showed a good correlation with the PWV changes, and the equations of the regression lines were $\Delta PWV = 7.258 \times \Delta SBP$ ($r=0.889$) and $\Delta PWV = 10.308 \times \Delta DBP$ ($r=0.912$), respectively. However, mean BP (MBP) changes showed the best correlation with PWV changes. The equation of the regression line was $\Delta PWV = 10.114 \times \Delta MBP$ ($r=0.913$) or $\%\Delta PWV = 0.719 \times \%\Delta MBP$ ($r=0.926$) (Fig. 1A). The changes in MBP and PWV were also well correlated in all-data analysis (Fig. 1B), but the changes in heart rate were not correlated with PWV changes ($r=0.059$, $p=0.48$). The equation of the regression line was $\Delta PWV = 7.901 \times \Delta MBP$ ($r=0.868$). MBP, but not heart rate, was a significant independent variable for PWV in multivariate regression analysis.

Long-Term Treatment

Benidipine treatment achieved stable BP control within 3 months, which was maintained until the end of the study. The average dose of benidipine at 12 months was 6.7 mg/day (4 mg for 3 patients and 8 mg for 6 patients). After 6 months, while PWV was also decreased significantly, heart rate was unchanged throughout the study (Table 1). We compared real (r-PWV) and estimated PWV (e-PWV) changes calculated from the BP decreases using the above regression formula. After 3 months, r-PWV and e-PWV showed almost the same degree of change, but the r-PWV value exceeded the e-PWV after 6 months, and the difference between r-PWV and e-PWV reached significance at 12 months (Fig. 2). The same trend was observed when BP and PWV changes were calculated as % changes (−17.4±2.3% for r-PWV *vs.* −12.3±1.2% for e-PWV; $p=0.028$ at 12 months). The trend became clearer when e-PWV was calculated using another formula derived from analysis of all-data (Fig. 2). Data concerning blood samples are summarized in Table 1. Interestingly, C-reactive protein (CRP) was decreased after benidipine treatment. As indicated in Table 1, other factors were not changed. Blood glucose and lipids including triglyceride, total cholesterol, high-density lipoprotein cholesterol and remnant-like lipoprotein cholesterol were also not changed (data not shown).

After suspension of benidipine for 2 weeks, BP and PWV were increased. However, these BP and PWV values remained significantly lower than the control values (Table 1). CRP was also increased after suspension of benidipine and was no longer significantly different from the control level.

Discussion

The fully automated waveform analyzer (form PWV/ABI) can measure baPWV non-invasively and quickly, and thus has been deployed in clinical practice. The baPWV is composed of a central elastic artery component and a peripheral muscular artery component. The PWV of the peripheral arteries is greater than that of the central arteries; therefore baPWV is considerably faster than authentic carotid-femoral PWV (*7*). baPWV values correlated well with carotid-femoral PWV, but the two parameters did not match completely (*7*). Although there are some differences between the two techniques, baPWV closely correlates with BP and age of subjects and reflects risk or progression of cardiovascular disease, as does carotid-femoral PWV (*4–9*). The most interesting and attractive characteristic of baPWV is, however, its rapid and large response to anti-hypertensive therapy, with significant decreases in baPWV being observed within 1 month after therapy (*12*). Thus, the baPWV is convenient to measure, is well correlated with organ damage and is a suitable index for monitoring arterial wall stiffness. Potentially, therefore, the baPWV may represent a useful new marker of the efficacy of anti-hypertensive therapy.

We examined the acute response of baPWV during hypotension induced by intravenous administration of nicardipine, which is the sole intravenously applicable dihydropyridine CAB in Japan. Acute changes in baPWV are mainly dependent on BP, though they may be affected to a lesser degree by heart rate (*19*), and are independent of arterial sclerosis. Regression analysis indicated that the decrease in baPWV achieved with CAB treatment was 10 times that of MBP, or about 0.7 times the % change in MBP (Fig. 1). The impact of our data is not negligible, because our estimated influence of BP changes on baPWV was much larger than that previously reported by Ichihara *et al.* (*10*). In their study, the change in the ratio of baPWV/MBP in response to various anti-hypertensive drugs was between 3.9 and 5.9, *vs.* 10.1 in our formula. Thus, this formula could account for most of the BP influence on baPWV. However, it has been reported that angiotensin-converting enzyme inhibitors or angiotensin-II receptor antagonists caused larger baPWV reductions than CAB, for a given BP reduction (*11*). Therefore, the formula cannot be applied as an absolute universal standard in cases involving anti-hypertensive treatments, but it does constitute a relative guide for baPWV monitoring. Furthermore, the formula cannot be applied to correction of the influence of BP in untreated hypertensive patients, because anti-hypertensive therapy alters hemodynamic and humoral states, and may alter reactivity of the vascular wall. Indeed, while the importance of raw baPWV values is undeniable, one must be careful in interpreting baPWV changes in anti-hypertensive

treatment.

The principal finding of our study was that baPWV progressively improved during long-term successful anti-hypertensive treatment with benidipine. The improvement was maintained following correction for BP changes, after 6 months of treatment (Fig. 2). Moreover, baPWV and BP remained at lower levels 2 weeks after suspension of benidipine (Table 1). These findings strongly suggest that the arterial properties of patients are improved by benidipine in conjunction with prolonged successful BP reduction. Benetos *et al.* (*20*) reported that PWV increases with age even in normotensive subjects and that the increase is greatly accelerated by co-existing high BP, high heart rate and high serum creatinine. Ichihara *et al.* (*10*) also reported significant reductions of baPWV following intensive BP lowering in a group of hypertensive patients, but not in a group undergoing moderate BP lowering. These findings, as well as those of the present study, highlight the importance of good control of BP for preventing or reversing the hypertension-induced progression of arterial stiffness.

Benidipine and nicardipine bear a close resemblance in the clinical setting; in a multi-center trial in Japan, the two drugs demonstrated comparable BP lowering capacity and minimal influence on pulse rate (*21*, *22*). Benidipine, however, seems to have a higher efficacy than nicardipine in coronary and glomerular arteries (*23*, *24*). In addition to BP lowering capacity, benidipine has beneficial effects on the vascular wall: benidipine improves endothelial function *via* stimulation of nitric oxide synthesis and inhibition of endothelin-1 expression (*16*, *18*, *25*). Benidipine also has an anti-oxidative action in hypertensive patients that could contribute to the prevention of arterial sclerosis (*26*). In addition, the ratio of baPWV reduction to BP lowering by benidipine in the present study was larger than those in previous reports (*10*, *11*). Thus, additional benefits of benidipine may include a contribution to the improvement of arterial properties, but further study is needed to confirm this. CRP is thought to be a predictive, causal and therapeutic marker of cardiovascular disease (*27*, *28*), and a decrease in CRP levels has been associated with good outcomes (*28*). Interestingly, CAB has been shown to improve endothelial function in association with CRP decreases in the coronary circulation (*29*). In the present study, the decrease in CRP levels after benidipine treatment may suggest an improvement in vascular function that could have been of some benefit to the patients.

In conclusion, we have confirmed the influence of BP on baPWV in patients undergoing anti-hypertensive therapy. In that context, benidipine relieved arterial stiffness after long-term reduction in BP. Monitoring baPWV in hypertensive patients is convenient and provides useful information about the state of the arterial wall, and with further study may be applicable to estimation of cardiovascular risk.

References

1. Laurent S, Boutouyrie P, Asmar R, *et al*: Aortic stiffness is an independent predictor of all-cause and cardiovascular mortality in hypertensive patients. *Hypertension* 2001; **37**: 1236–1241.
2. Blacher J, Asmar R, Djane S, London GM, Safar ME: Aortic pulse wave velocity as a marker of cardiovascular risk in hypertensive patients. *Hypertension* 1999; **33**: 1111–1117.
3. Guerin AP, Blacher J, Pannier B, Marchais SJ, Safar ME, London ME: Impact of aortic stiffness attenuation on survival of patients in end-stage renal failure. *Circulation* 2001; **103**: 987–992.
4. Kita T, Kitamura K, Hashida S, Morishita K, Eto T: Plasma adrenomedullin is closely correlated with pulse wave velocity in middle-aged and elderly patients. *Hypertens Res* 2003; **26**: 887–893.
5. Imanishi R, Seto S, Toda G, *et al*: High brachial-ankle pulse wave velocity is an independent predictor of the presence of coronary artery disease in men. *Hypertens Res* 2004; **27**: 71–78.
6. Koji Y, Tomiyama H, Ichihashi H, *et al*: Comparison of ankle-brachial pressure index and pulse wave velocity as markers of the presence of coronary artery disease in subjects with a high risk of atherosclerotic cardiovascular disease. *Am J Cardiol* 2004; **94**: 868–872.
7. Munakata M, Ito N, Nunokawa T, Yoshinaga K: Utility of automated brachial ankle pulse wave velocity measurements in hypertensive patients. *Am J Hypertens* 2003; **16**: 653–657.
8. Matsui Y, Kario K, Ishikawa J, Eguchi K, Hoshide S, Shimada K: Reproducibility of arterial stiffness indices (pulse wave velocity and augmentation index) simultaneously assessed by automated pulse wave analysis and their associated risk factors in essential hypertensive patients. *Hypertens Res* 2004; **27**: 851–857.
9. Munakata M, Sakuraba J, Tayama J, *et al*: Higher brachial-ankle pulse wave velocity is associated with more advanced carotid atherosclerosis in end-stage renal disease. *Hypertens Res* 2005; **28**: 9–14.
10. Ichihara A, Hayashi M, Koura Y, Toda Y, Hirota N, Saruta T: Long-term effects of intensive blood pressure lowering on arterial wall stiffness in hypertensive patients. *Am J Hypertens* 2003; **16**: 959–965.
11. Munakata M, Nagasaki A, Nunokawa T, *et al*: Effects of valsartan and nifedipine coat-core on systemic arterial stiffness in hypertensive patients. *Am J Hypertens* 2004; **17**: 1050–1055.
12. Agata J, Nagahara D, Kinoshita S, *et al*: Angiotensin II receptor blocker prevents increased arterial stiffness in patients with essential hypertension. *Circ J* 2004; **68**: 1194–1198.
13. Pitt B, Byington RP, Furberg CD, *et al*, PREVENT Investigators: Effect of amlodipine on the progression of atherosclerosis and the occurrence of clinical events. *Circulation* 2000; **102**: 1503–1510.
14. Zanchetti A, Bond MG, Henning M, *et al*: Calcium antagonist lacidipine slows down progression of asymptomatic carotid atherosclerosis: principal results of the European

Lacidipine Study on Atherosclerosis (ELSA), a randomized, double-blind, long-term trial. *Circulation* 2002; **106**: 2422–2427.
15. Nissen SE, Tuzcu EM, Libby P, *et al*: Effect of antihypertensive agents on cardiovascular events in patients with coronary disease and normal blood pressure: the CAMELOT study: a randomized controlled trial. *JAMA* 2004; **292**: 2217–2225.
16. Dohi Y, Kojima M, Sato K: Benidipine improves endothelial function in renal resistance arteries of hypertensive rats. *Hypertension* 1996; **28**: 58–63.
17. Kobayashi N, Kobayashi K, Kouno K, Yagi S, Matsuoka H: Effect of benidipine on microvascular remodeling and coronary flow reserve in two-kidney, one clip Goldblatt hypertension. *J Hypertens* 1997; **15**: 1285–1294.
18. Yamashita T, Kawashima S, Ozaki M, *et al*: A calcium channel blocker, benidipine, inhibits intimal thickening in the carotid artery of mice by increasing nitric oxide production. *J Hypertens* 2001; **19**: 451–458.
19. Wilkinson IB, Mohammad NH, Tyrrell S, *et al*: Heart rate dependency of pulse pressure amplification and arterial stiffness. *Am J Hypertens* 2002; **15**: 24–30.
20. Benetos A, Adamopoulos C, Bureau J-M, *et al*: Determinants of accelerated progression of arterial stiffness in normotensive subjects and in treated hypertensive subjects over 6-year period. *Circulation* 2002; **105**: 1202–1207.
21. National Intervention Cooperative Study in Elderly Hypertension Study Group: Randomized double-blind comparison of a calcium antagonist and a diuretic in elderly hypertensives. *Hypertension* 1999; **34**: 1129–1133.
22. Tsukiyama H, Kikawada R, Osada H, *et al*: Safety and efficacy of long-term therapy with benidipine in aged hypertensive patients. *Geriat Med* 1997; **35**: 989–1007 (in Japanese).
23. Ito A, Fukumoto Y, Shimokawa H: Changing characteristics of patients with vasospastic angina in the era of new calcium channel blockers. *J Cardiovasc Pharmacol* 2004; **44**: 480–485.
24. Hayashi K, Ozawa Y, Fujiwara K, Wakino S, Kumagai H, Saruta T: Role of actions of calcium antagonists on efferent arterioles—with special references to glomerular hypertension. *Am J Nephrol* 2003; **23**: 229–244.
25. Kobayashi N, Nakano S, Mori Y, Kobayashi T, Tsubokou Y, Matsuoka H: Benidipine inhibits expression of ET-1 and TGF-β1 in Dahl salt-sensitive hypertensive rats. *Hypertens Res* 2001; **24**: 241–250.
26. Yasunari K, Maeda K, Nakamura M, Watanabe T, Yoshikawa J: Benidipine, a long-acting calcium channel blocker, inhibits oxidative stress in polymorphonuclear cells in patients with essential hypertension. *Hypertens Res* 2005; **28**: 107–112.
27. Pai JK, Pischon T, Ma J, *et al*: Inflammatory markers and the risk of coronary heart disease in men and women. *N Engl J Med* 2004; **351**: 2599–2610.
28. Ridker PM, Cannon CP, Morrow D, *et al*: C-reactive protein levels and outcomes after statin therapy. *N Engl J Med* 2005; **352**: 20–28.
29. Takase H, Toriyama T, Sugiyama M, *et al*: Effect of nifedipine on C-reactive protein levels in the coronary sinus and on coronary blood flow in response to acetylcholine in patients with stable angina pectoris having percutaneous coronary intervention. *Am J Cardiol* 2005; **95**: 1235–1237.

ELSEVIER

Cardiovascular Research 70 (2006) 158 – 164

Cardiovascular Research

www.elsevier.com/locate/cardiores

Adrenomedullin in mast cells of abdominal aortic aneurysm

Toshihiro Tsuruda [a,b,*], Johji Kato [a], Kinta Hatakeyama [c], Atsushi Yamashita [c], Kunihide Nakamura [d], Takuroh Imamura [a], Kazuo Kitamura [a], Toshio Onitsuka [d], Yujiro Asada [c], Tanenao Eto [a]

[a] *First Department of Internal Medicine, Miyazaki Medical College, University of Miyazaki, Japan*
[b] *Department of Nutrition Management, Faculty of Health and Nutrition, Minami-Kyushu University, Japan*
[c] *Department of Pathology, Miyazaki Medical College, University of Miyazaki, Japan*
[d] *Second Department of Surgery, Miyazaki Medical College, University of Miyazaki, Japan*

Received 24 September 2005; received in revised form 26 January 2006; accepted 1 February 2006
Available online 9 March 2006
Time for primary review 22 days

Abstract

Objectives: Produced by vascular walls, adrenomedullin (AM) exerts antifibrotic actions in the process of cardiovascular remodeling. The purpose of this study was to examine the pathophysiological role of AM in the development of human abdominal aortic aneurysm (AAA).
Methods and results: Immunohistochemical analyses revealed that vascular smooth muscle cells in the media were positive for AM in the early stage of atherosclerotic aorta. Intense immunoreactivity was observed in mast cells of the outer media and adventitia of AAA, and the number of mast cells was greater ($p<0.01$) in AAA than in atherosclerotic aorta without any aneurysmal change. To determine the role of AM in mast cells, we examined cultured human mast cell leukemia line-1 (HMC-1) and fibroblasts isolated from AAA patients. Cultured HMC-1 cells were found to express preproAM gene and release AM peptide into the cultured media. When assessed by collagenase-sensitive [^{3}H]proline incorporation and procollagen type I C-peptide secretion, collagen synthesis in co-culture of HMC-1 and the fibroblasts was reduced by 10^{-6} mol/L synthetic AM, while conversely, it increased following blockade of the action of endogenous AM with 10 μg/mL anti-AM monoclonal antibody.
Conclusion: The present study suggests an anti-fibrotic role for AM released from mast cells, providing new insight into the biological actions of mast cell-derived AM in the development of AAA.

Keywords: Adrenomedullin; Abdominal aortic aneurysm; Mast cell; Fibrosis

1. Introduction

Abdominal aortic aneurysm (AAA) is a relatively common disorder in elderly patients with atherosclerosis [1,2]. AAA is characterized by an enlarged aortic lumen with a degenerated medial layer that is rearranged by disorganized collagen fibers, and in addition, either fibroblast proliferation with extracellular matrix formation or chronic inflammatory cellular infiltration is often observed in the outer media and adventitia [3]. A number of factors have been proposed as the cause of AAA [4–6]; however, the mechanisms underlying the development of the aneurysm remain unknown.

Adrenomedullin (AM), a 52-amino acid peptide originally isolated from human pheochromocytoma [7], has been shown to exert a wide range of cardiovascular actions, which are mostly protective for blood vessels, such as stimulation of nitric oxide production and inhibitions of oxidative stress and endothelial cell apoptosis [8]. Expression of the AM peptide was observed in the myocardium and in the vascular wall [9], suggesting a role for AM as a locally-acting humoral factor [10,11]. The magnitude of fibrosis of the cardiac or vascular tissues is determined by

* Corresponding author. First Department of Internal Medicine, Miyazaki Medical College, University of Miyazaki, 5200 Kihara Kiyotake, Miyazaki 889-1692, Japan. Tel.: +81 985 85 0872; fax: +81 985 85 6596.
E-mail address: ttsuruda@med.miyazaki-u.ac.jp (T. Tsuruda).

0008-6363/$ - see front matter © 2006 European Society of Cardiology. Published by Elsevier B.V. All rights reserved.
doi:10.1016/j.cardiores.2006.02.003

not only the mechanical stress but also the balance of humoral factors [12]. We have so far reported inhibitory effects of AM on fibroblast proliferation and extracellular matrix formation using cultured cells in vitro [13,14] and rodent models for hypertensive heart disease and myocardial infarction in vivo [15,16]. Based upon previous studies, we hypothesized that AM is involved in the development of AAA through modulation of fibroblast proliferation or extracellular matrix formation.

In the first part of the present study, to examine the role of AM in AAA, we characterized its expression in the aneurysmal aorta obtained from patients with AAA on surgical repair, and found that AM was present in mast cells in the outer media and adventitia. In the second part, we explored whether or not mast cell-derived AM modulates production of the extracellular matrix, by using a human mast cell line and cultured human fibroblasts isolated from the AAA tissue.

2. Materials and methods

The present study is approved by the Human Investigation Review Committee of the University of Miyazaki (Nos. 99 and 177) and conforms with the principles outlined in the Declaration of Helsinki (*Cardiovasc Res* 1997; 35: 2–4).

2.1. Reagents

Synthetic human AM was purchased from Peptide Institute, Inc. (Osaka, Japan). Dulbecco's modified Eagle's medium (DMEM)/F-12, Iscove's modified Dulbecco's medium, fetal bovine serum and antibiotics were obtained from GIBCO BRL. Collagenase (type IV) and insulin-transferrin-sodium selenite media supplement were from Sigma.

2.2. Tissue preparation

Aneurysmal tissues was obtained from the anterior part of aortic walls of 28 patients with AAA associated with atherosclerosis (75±1 years; male, 71%) during elective repair surgery with written informed consent. The AAA tissues were fixed in 10% formalin immediately after resection. Aortic tissues with various degrees of atherosclerosis were collected from the anterior part of aorta of 20 patients (64±3 years; male, 80%) at autopsy performed within 6 h post-mortemly. Tissues of 10 of them showed diffuse intimal thickening or fatty streak and those of 10 advanced atherosclerosis.

2.3. Cell culture

Cultured fibroblasts were isolated from aorta of patients with AAA as described previously with minor modification [13]. In brief, minced aortic tissues digested with 0.12% trypsin and 0.03% collagenase type IV were placed in DMEM/F-12 medium with 10% fetal bovine serum in 10-cm culture plates for 2 h at 37 °C, and the adherent cells were further incubated until confluent. The human mast cell leukemia line, HMC-1, was kindly provided by Dr. J.H. Butterfield (Mayo Clinic, Rochester, MN, USA) [17] and cultured in Iscove's modified Dulbecco's medium.

2.4. Immunohistochemical analysis

Aortic tissues fixed in 10% formalin and embedded in paraffin wax. Sections (3 μm thick) were immunohistochemically examined as previously described [18], with monoclonal antibodies against human α-smooth muscle actin or tryptase (DAKO cytomation) or with anti-human AM monoclonal antibody [19,20]. For detection of mast cell tryptase, the tissue sections were microwaved at 95 °C for 1.0 h in 10 mmol/L citrate buffer (pH 6.0) prior to incubation with the primary antibody. As a negative control, non-immune IgG of mouse was used instead of the primary antibodies. Mast cell numbers of at least 6 fields in total areas of the outer-media and adventitia in atherosclerosis and AAA were counted at the magnification of ×400 and expressed as a density of mast cell number per mm^2. The intracellular localization of AM and tryptase in HMC-1 cells was evaluated by double immunofluorescence staining with the anti-human AM antibody and goat anti-human tryptase polyclonal antibody (Santa Cruz Biotechnology) overnight at 4 °C, followed by staining with fluorescein isothiocyanate-conjugated anti-mouse IgG and Cy3-conjugated anti-goat IgG (Jackson ImmunoResearch) for 20 min. Immunofluorescent images were analyzed with a spectral confocal scanning system (TCS SP2, Leica).

2.5. Gene expression and assay for AM

Gene expression of AM in total RNA isolated from HMC-1 was analyzed by using a reverse transcription-polymerase chain reaction (RT-PCR) method [15,21]. The amplification protocol was 94 °C for 2 min, then 26 cycles of 94 °C for 30 s, 62 °C for 30 s and 72 °C for 1 min, and finally 72 °C for 5 min. The PCR products were electrophoresed on 3.0% agarose gel with ethidium bromide. The concentration of AM in the conditioned medium as well as in the cells was measured with an immunoenzymometric assay, as previously described [22].

2.6. Measurement of collagen synthesis de novo

The synthesis of collagen de novo was assessed by collagen-sensitive proline incorporation into the cells [23,24] and by procollagen type I C-peptide (PICP), a peptide cleaved from the carboxy terminus of procollagen type I during posttranslational processing into the collagen fibers [25], in the conditioned medium. After the confluent fibroblasts were incubated with serum-free DMEM/F-12

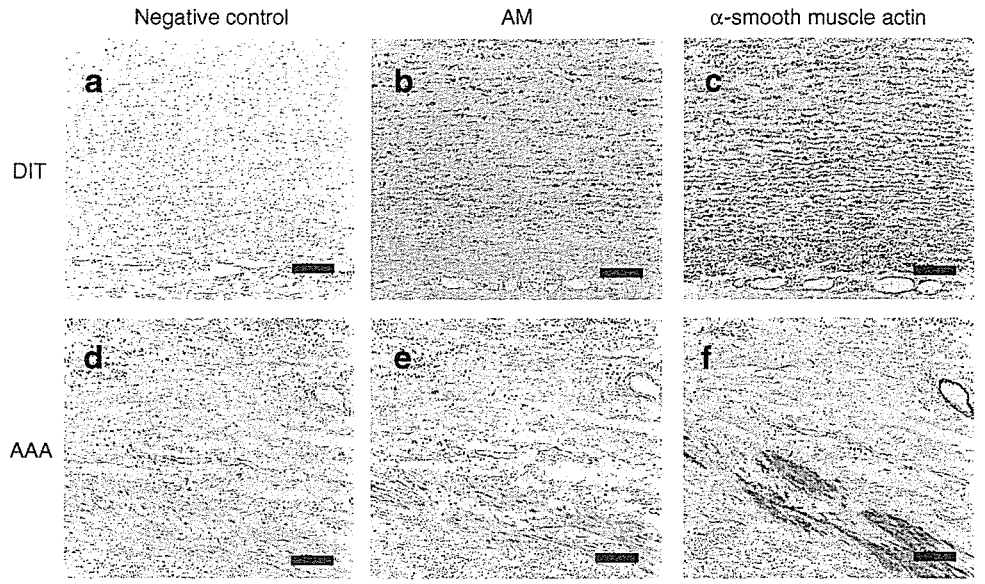

Fig. 1. Localization of immunoreactive AM (b and e) or α-smooth muscle actin (c and f) and negative control (a and d) of aortic tissues with AAA (d–f) and with diffuse intimal thickening (DIT, a–c). Bar, 100 μm.

medium for 48 h, HMC-1 cells (1×10^6/cm^3) were placed on the fibroblasts with or without of 10^{-6} mol/L synthetic AM in the absence or presence of 10 μg/mL purified anti-AM monoclonal antibody or purified non-immune mouse IgG (Zymed Laboratories, Inc., San Francisco, USA). To measure collagen-sensitive proline incorporation, the cultured cells were incubated with 5.0 μCi/mL of [^{3}H]proline (Amersham Bioscience) for a further 24 h. The concentrations of PICP secreted in the conditioned media during the 24-h incubation with or without synthetic AM or anti-AM antibody were determined with commercially available enzyme immunoassay (Takara).

2.7. Statistical analysis

All data were analyzed with the SPSS software of version 11.0 (SPSS Inc., Chicago, IL) and expressed as the median with the 10–90% range and extreme values. Two data were

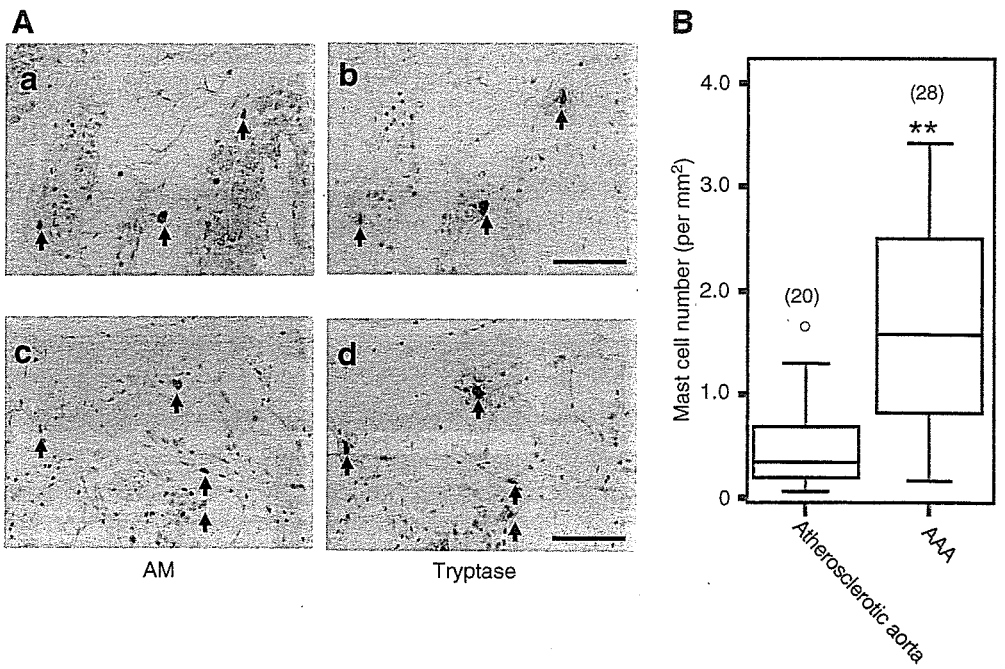

Fig. 2. (A) Localization of immunoreactive AM (a and c) and tryptase (b and d) of two serial sections of AAA. Arrows indicate mast cells positive for AM or tryptase. Bar, 100 μm. (B) Number of mast cells in atherosclerotic aorta and AAA. Mast cells immunostained with anti-human mast cell tryptase antibody were counted at magnification of ×400 under the microscope. Values are shown as the median with 10–90% range (n); $^{**}p < 0.01$, vs. atherosclerotic aorta.

compared with Student's t-test, and comparisons among multiple groups were assessed with a one-way ANOVA followed by Sheffè's test. Statistical significance was accepted at $p<0.05$.

3. Results

3.1. Localization of immunoreactive AM

Fig. 1 illustrates the immunoreactive localization for AM and α-smooth muscle actin in the aortic walls of AAA or of diffuse intimal thickening. In the aneurysmal wall, immunoreactivity for AM was detected in the degenerated media replaced by fibrous tissues, where the residual smooth muscle cells, mural vessels, and fibroblast-like cells were weakly stained. In the aortic wall with diffuse intimal thickening, immunoreactivity for AM was located mainly in the media.

3.2. Immunoreactivity for AM in mast cells of AAA

We further examined the aortic sections from AAA patients stained with anti-AM monoclonal antibody. Fig. 2A illustrates the representative localizations of immunoreactive AM and tryptase in the adventitia of AAA. The immunoreactivity for AM was abundantly present in the cells located in connective tissue, which were identified as mast cells in the serial sections, based on positive staining for tryptase, a specific marker for mast cells. Next, a comparison was made of the number of mast cells between the aortic tissues with and without AAA. As shown in Fig. 2B, the number of mast cells was significantly ($p<0.01$) increased in the outer media and adventitia in cases of AAA, compared to atherosclerotic aorta without AAA.

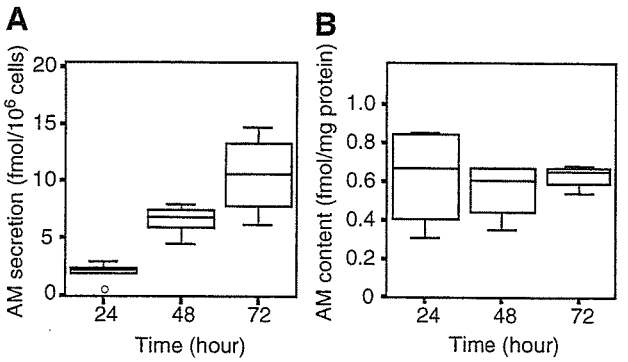

Fig. 4. (A) Secretion of AM from HMC-1 cells into the conditioned media. (B) Intracellular concentration of AM in HMC-1 cells. HMC-1 cells were cultured in serum-free media for the indicated time period. Values are shown as the median with 10–90% range and the numbers of samples are 4–7 for secretion and 4 for AM content measurements.

3.3. AM production in mast cell line

We examined the human mast cell leukemia line HMC-1 to see whether or not mast cells can produce and secrete AM. RT-PCR revealed expression of the preproAM gene in cultured HMC-1 cells (Fig. 3A), and immunohistochemical studies showed that AM (green) and tryptase (red) were positive in a granular pattern, co-localizing partially in merging images (yellow) (Fig. 3B). As shown in Fig. 4A, HMC-1 cells secreted AM into the medium in a time-dependent manner for up to 72 h, with unchanged intracellular AM levels (Fig. 4B). To examine the molecular forms of secreted AM, we analyzed immunoreactive AM secreted from co-culture of the mast cells and fibroblasts over an incubation period of 24 h with reverse phase high-performance liquid chromatography (RP-HPLC). The RP-HPLC analysis showed that immunoreac-

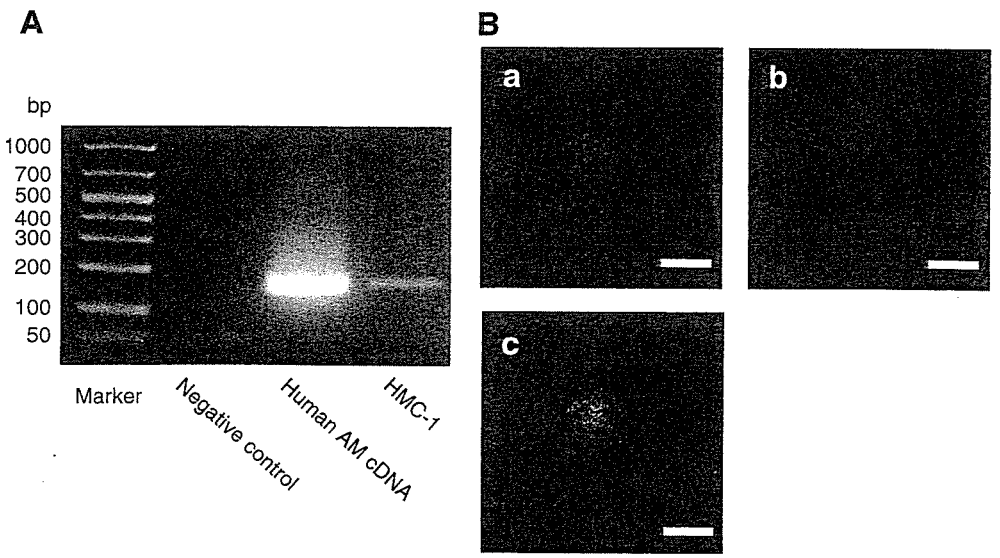

Fig. 3. (A) Expression of preproAM mRNA in the HMC-1 cell line. (B) Localization of immunoreactive AM (a, green) or tryptase (b, red) and a merged image (c, yellow) in HMC-1 cells. Bar, 10 μm.

tive AM consisted of a single peak eluting at the position of human AM(1–52)-NH_2.

3.4. Effect of AM on protein and collagen synthesis

Fig. 5 shows the effects of exogenous and endogenous AM on collagenase-sensitive proline incorporation (A), PICP level in the conditioned media (B) and cellular protein content (C) of cultured HMC-1 cells and fibroblasts isolated from aorta with AAA. Although AM had little effect on the total protein content, 10^{-6} mol/L AM significantly ($p<0.05$) decreased the proline incorporation and PICP level in co-culture of HMC-1 and fibroblasts. In contrast, blockade of the action of endogenous AM with 10 μg/mL of purified anti-AM monoclonal antibody resulted in increased proline incorporation and PICP level.

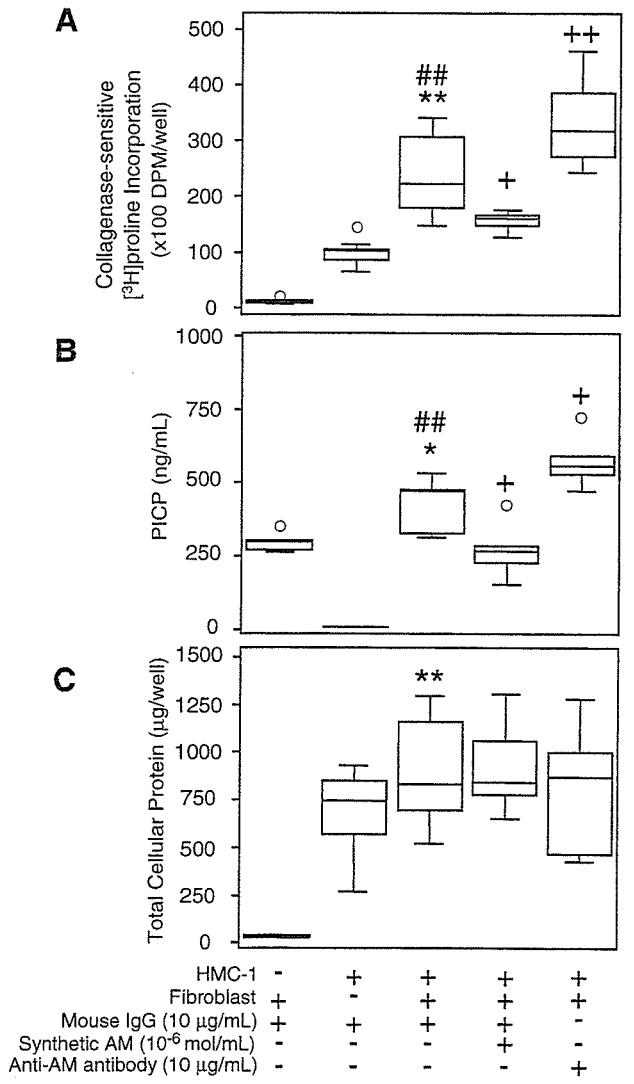

Fig. 5. [^{3}H]proline incorporation (A), procollagen type I C-peptide (PICP) (B) and cellular protein levels (C) of co-culture of HMC-1 cells and fibroblasts incubated with or without 10^{-6} mol/L synthetic AM in the absence or presence of 10 μg/mL purified anti-AM monoclonal antibody or 10 μg/mL purified non-immune mouse IgG. *Values are shown as the median with 10–90% range*, and the number of samples are 8–12 for proline incorporation, 6 for PICP and 6 for cellular protein. $^{*}p<0.05$, $^{**}p<0.01$, vs. fibroblasts alone; $^{\#\#}p<0.01$, vs. HMC-1 alone; $^{+}p<0.05$, $^{++}p<0.01$ vs. control co-culture of fibroblasts and HMC-1 cells.

4. Discussion

Here, we demonstrated the presence of AM in mast cells of the outer media and adventitia of patients with AAA as well as in the human mast cell line HMC-1. Second, AM was released from HMC-1 and suppressed the synthesis of collagen in co-culture of HMC-1 cells and fibroblasts in vitro. The present study suggests a role for mast cell-derived AM in modulating production of the extracellular matrix of AAA.

AM has been reported to be found in various tissues and organs [9], but in particular, locally produced AM in the heart and vasculature has gained attention because of its role as an autocrine or paracrine factor [10,11]. AM exerted anti-fibrotic effects on the heart and blood vessels in vitro and in vivo, attenuating myofibroblastic differentiation and collagen synthesis and stimulating matrix metalloproteinase-2 (MMP-2) activity [14,15]. In the present study, the medial and adventitial layers of the aortic aneurysmal wall were replaced by fibrous tissue, where the residual smooth muscle cells and fibroblast-like cells were weakly positive for AM. Unexpectedly, during the microscopic observation, intense immunoreactivity for AM was observed in mast cells, number of which markedly increased in the outer media and adventitia of AAA. In accord with this, the cultured mast cell line was found to express preproAM mRNA and to contain the AM peptide in the secretory granules.

Accumulation of mast cells is observed in fibrotic tissues of idiopathic cardiomyopathy [26] and of vascular walls with atherosclerotic changes [27], suggesting a potential role of this type of cells in the pathogenesis. Mast cells can directly exert fibrogenic effects by releasing or activating several mediators such as histamine and tryptase [28,29]. To look at the role of AM on extracellular matrix formation in the aneurysmal walls, we treated co-culture of the mast cells and fibroblasts with synthetic AM or purified anti-AM monoclonal antibody which binds to the ring structure, critical for the biological activity of this peptide. When assessed with collagenase-sensitive proline incorporation and with PICP secretion, collagen synthesis de novo in the cells was reduced by synthetic AM, while conversely, increased by the blockade of action of endogenous AM by the anti-AM antibody. These results clearly suggest an inhibitory action of exogenous and endogenous AM on collagen synthesis in the cultured cells. The intracellular mechanisms of action for AM are not completely understood, while accumulation of intracellular cAMP has been proposed as a mechanism [7,8]. Indeed, AM has been shown to inhibit collagen synthesis via elevation of cAMP levels in cultured fibroblasts [30] and this mechanism is

considered for the AM action observed in the present cell-culture study.

Collagen deposition in tissues is determined not only by its production but also by enzymatic degradation, and AM was found to augment MMP-2 activity in cultured aortic adventitial fibroblasts of rats [14]. We therefore measured MMP-2 activity in conditioned media of the mast cells and fibroblasts, but found that neither synthetic AM nor anti-AM antibody had effect on the enzymatic activity (data not shown). Recently, Martínez et al. [31] reported cleavage of the AM peptide into smaller fragments by MMP-2; however RP-HPLC analysis showed that the major molecular form of AM secreted from the mast cells and fibroblasts was the full-length human AM(1–52)-NH_2. Therefore, it seems unlikely that the anti-fibrotic effect of exogenous or endogenous AM is modulated by alteration of MMP-2 activity.

The clinical significance of mast cells in the development of AAA has yet to be defined, though several studies have shown possible activation of chymase and matrix metalloproteinases by the cells [32,33]. In the present study, we observed a significant increase in mast cell number in the outer media and adventitia of AAA. As mentioned above, mast cells are assumed to release pro-fibrotic factors, compensating for the loss of structural integrity in the aneurysmal wall. According to the present experiments in vitro, AM released from mast cells may have potency to suppress deposition of extracellular matrix; however, it is unclear whether or not suppressed extracellular matrix formation by AM is beneficial in preventing AAA from enlarging. *Indeed, we found no significant correlation between the AM levels and collagen contents or wall thickness of the AAA tissues (data not shown), partly because of the limited number of samples or of the removal of intima or part of media during the operation.* Thus, further studies, particularly in vivo, are needed to answer this important question.

In summary, AM was found to be produced by mast cells in the outer media and adventitia of AAA, and the cell culture experiments showed an anti-fibrotic action of AM released from a human mast cell line. This study provides new insight into the biological action of mast cell-derived AM in modulating formation of the extracellular matrix in the development of AAA.

Acknowledgements

This study was supported by grants-in-aid for Scientific Research on Priority Areas and for the 21st Century Centers of Excellence Program (Life Science) from the Ministry of Education, Culture, Sport, Science and Technology, Japan, a grant-in-aid from the Suzuken Memorial Foundation, the Mochida Memorial Foundation for Medical and Pharmaceutical Research, and an incentive grant from Minami-Kyushu University. We are thankful to Dr. J.H. Butterfield, Mayo Clinic, Rochester, MN, USA for providing the mast cell line HMC-1. We also thank Drs. Kazushi Kojima, Mitsuhiro Yano, Yoshikazu Yano, Second Department of Surgery for their help to collect the AAA samples, Drs. Fukumi Nakamura-Uchiyama and Yukifumi Nawa, Department of Parasitology, Dr. Kousuke Marutsuka, Department of Pathology, University of Miyazaki for their helpful discussion, and Ms. Ritsuko Sotomura and Ms. Mariko Tokashiki for their technical assistance.

References

[1] Hallett Jr JW. Management of abdominal aortic aneurysms. Mayo Clin Proc 2000;75:395–9.
[2] Brady AR, Fowkes FG, Thompson SG, Powell JT. Aortic aneurysm diameter and risk of cardiovascular mortality. Arterioscler Thromb Vasc Biol 2001;21:1203–7.
[3] Rosai J. Cardiovascular system. In: Rosai, editor. Rosai and Ackerman's surgical pathology, 9th ed. Philadelphia: Elsevier Inc; 2004. p. 2438–9.
[4] Lindholt JS, Støvring J, Østergaard L, Urbonavicius S, Henneberg EW, Honoré B, et al. Serum antibodies against Chlamydia pneumoniae outer membrane protein cross-react with the heavy chain of immunoglobulin in the wall of abdominal aortic aneurysms. Circulation 2004;109:2097–102.
[5] Freestone T, Turner RJ, Coady A, Higman DJ, Greenhalgh RM, Powell JT. Inflammation and matrix metalloproteinases in the enlarging abdominal aortic aneurysm. Arterioscler Thromb Vasc Biol 1995;15:1145–51.
[6] Leskinen M, Wang Y, Leszczynski D, Lindstedt KA, Kovanen PT. Mast cell chymase induces apoptosis of vascular smooth muscle cells. Arterioscler Thromb Vasc Biol 2001;21:516–22.
[7] Kitamura K, Kangawa K, Kawamoto M, Ichiki Y, Nakamura S, Matsuo H, et al. Adrenomedullin: a novel hypotensive peptide isolated from human pheochromocytoma. Biochem Biophys Res Commun 1993;192:553–60.
[8] Kato J, Tsuruda T, Kita T, Kitamura K, Eto T. Adrenomedullin: a protective factor for blood vessels. Arterioscler Thromb Vasc Biol 2005;12:2480–7.
[9] Eto T, Kato J, Kitamura K. Regulation of production and secretion of adrenomedullin in the cardiovascular system. Regul Pept 2003;112: 61–9.
[10] Kato J, Tsuruda T, Kitamura K, Eto T. Adrenomedullin: a possible autocrine or paracrine hormone in the cardiac ventricles. Hypertens Res 2003;26:S113–9.
[11] Tsuruda T, Burnett Jr JC. Adrenomedullin: an autocrine/paracrine factor for cardiorenal protection. Circ Res 2002;90:625–7.
[12] Weber KT. Targeting pathological remodeling: concepts of cardioprotection and reparation. Circulation 2000;102:1342–5.
[13] Tsuruda T, Kato J, Kitamura K, Kawamoto M, Kuwasako K, Imamura T, et al. An autocrine or a paracrine role of adrenomedullin in modulating cardiac fibroblast growth. Cardiovasc Res 1999;43: 958–67.
[14] Tsuruda T, Kato J, Cao YN, Hatakeyama K, Masuyama H, Imamura T, et al. Adrenomedullin induces matrix metalloproteinase-2 activity in rat aortic adventitial fibroblasts. Biochem Biophys Res Commun 2004;325:80–4.
[15] Tsuruda T, Kato J, Hatakeyama K, Masuyama H, Cao YN, Imamura T, et al. Antifibrotic effect of adrenomedullin on coronary adventitia in angiotensin II-induced hypertensive rats. Cardiovasc Res 2005; 65:921–9.
[16] Nakamura R, Kato J, Kitamura K, Onitsuka H, Imamura T, Cao Y, et al. Adrenomedullin administration immediately after myocardial infarction ameliorates progression of heart failure in rats. Circulation 2004;110:426–31.

[17] Butterfield JH, Weiler D, Dewald G, Gleich GJ. Establishment of an immature mast cell line from a patient with mast cell leukemia. Leuk Res 1988;12:345–55.
[18] Ishikawa T, Hatakeyama K, Imamura T, Ito K, Hara S, Date H, et al. Increased adrenomedullin immunoreactivity and mRNA expression in coronary plaques obtained from patients with unstable angina. Heart 2004;90:1206–10.
[19] Marutsuka K, Hatakeyama K, Sato Y, Yamashita A, Sumiyoshi A, Asada Y. Immunohistological localization and possible functions of adrenomedullin. Hypertens Res 2003;26:S33–40.
[20] Ohta H, Tsuji T, Asai S, Sasakura K, Teraoka H, Kitamura K, et al. One-step direct assay for mature-type adrenomedullin with monoclonal antibodies. Clin Chem 1999;45:244–51.
[21] Uemura T, Kato J, Kuwasako K, Kitamura K, Kangawa K, Eto T. Aldosterone augments adrenomedullin production without stimulating pro-adrenomedullin N-terminal 20 peptide secretion in vascular smooth muscle cells. J Hypertens 2002;20:1209–14.
[22] Kita T, Kitamura K, Hashida S, Morishita K, Eto T. Plasma adrenomedullin is closely correlated with pulse wave velocity in middle-aged and elderly patients. Hypertens Res 2003;26:887–93.
[23] Ostrom RS, Naugle JE, Hase M, Gregorian C, Swaney JS, Insel PA, et al. Angiotensin II enhances adenylyl cyclase signaling via Ca^{2+}/calmodulin. Gq-Gs cross-talk regulates collagen production in cardiac fibroblasts. J Biol Chem 2003;278:24461–8.
[24] Tsuruda T, Boerrigter G, Huntley BK, Noser JA, Cataliotti A, Costello-Boerrigter LC, et al. Brain natriuretic peptide is produced in cardiac fibroblasts and induces matrix metalloproteinases. Circ Res 2002;91:1127–34.
[25] Taubman MB, Goldberg B, Sherr C. Radioimmunoassay for human procollagen. Science 1974;186:1115–7.
[26] Patella V, Marinò I, Arbustini E, Lamparter-Schummert B, Verga L, Adt M, et al. Stem cell factor in mast cells and increased mast cell density in idiopathic and ischemic cardiomyopathy. Circulation 1998; 97:971–8.
[27] Atkinson JB, Harlan CW, Harlan GC, Virmani R. The association of mast cells and atherosclerosis: a morphologic study of early atherosclerotic lesions in young people. Hum Pathol 1994;25:154–9.
[28] Levi-Schaffer F, Piliponsky AM. Tryptase, a novel link between allergic inflammation and fibrosis. Trends Immunol 2003;24:158–61.
[29] Garbuzenko E, Nagler A, Pickholtz D, Gillery P, Reich R, Maquart FX, et al. Human mast cells stimulate fibroblast proliferation, collagen synthesis and lattice contraction: a direct role for mast cells in skin fibrosis. Clin Exp Allergy 2002;32:237–46.
[30] Horio T, Nishikimi T, Yoshihara F, Matsuo H, Takishita S, Kangawa K. Effects of adrenomedullin on cultured rat cardiac myocytes and fibroblasts. Eur J Pharmacol 1999;382:1–9.
[31] Martínez A, Oh HR, Unsworth EJ, Bregonzio C, Saavedra JM, Stetler-Stevenson WG, et al. Matrix metalloproteinase-2 cleavage of adrenomedullin produces a vasoconstrictor out of a vasodilator. Biochem J 2004;383:413–8.
[32] Tsunemi K, Takai S, Nishimoto M, Yuda A, Hasegawa S, Sawada Y, et al. Possible roles of angiotensin II-forming enzymes, angiotensin converting enzyme and chymase-like enzyme, in the human aneurysmal aorta. Hypertens Res 2002;25:817–22.
[33] Baram D, Vaday GG, Salamon P, Drucker I, Hershkoviz R, Mekori YA. Human mast cells release metalloproteinase-9 on contact with activated T cells: Juxtacrine regulation by TNF-α. J Immunol 2001; 167:4008–16.

THE JOURNAL OF BIOLOGICAL CHEMISTRY VOL. 281, NO. 11, pp. 7205–7213, March 17, 2006

Functions of the Cytoplasmic Tails of the Human Receptor Activity-modifying Protein Components of Calcitonin Gene-related Peptide and Adrenomedullin Receptors*[S]

Received for publication, October 13, 2005, and in revised form, January 6, 2006 Published, JBC Papers in Press, January 11, 2006, DOI 10.1074/jbc.M511147200

Kenji Kuwasako[‡1], Yuan-Ning Cao[‡], Chun-Ping Chu[§], Shuji Iwatsubo[‡], Tanenao Eto[‡], and Kazuo Kitamura[‡]

From the [‡]First and [§]Third Departments of Internal Medicine, Miyazaki Medical College, University of Miyazaki, Miyazaki 889-1692, Japan

Receptor activity-modifying proteins (RAMPs) enable calcitonin receptor-like receptor (CRLR) to function as a calcitonin gene-related peptide receptor (CRLR/RAMP1) or an adrenomedullin (AM) receptor (CRLR/RAMP2 or -3). Here we investigated the functions of the cytoplasmic C-terminal tails (C-tails) of human RAMP1, -2, and -3 (hRAMP1, -2, and -3) by cotransfecting their C-terminal deletion or progressive truncation mutants into HEK-293 cells stably expressing hCRLR. Deletion of the C-tail from hRAMP1 had little effect on the surface expression, function, or intracellular trafficking of the mutant heterodimers. By contrast, deletion of the C-tail from hRAMP2 disrupted transport of hCRLR to the cell surface, resulting in significant reductions in ^{125}I-hAM binding and evoked cAMP accumulation. The transfection efficiency for the hRAMP2 mutant was comparable with that for wild-type hRAMP2; moreover, immunocytochemical analysis showed that the mutant hRAMP2 remained within the endoplasmic reticulum. FACS analysis revealed that deleting the C-tail from hRAMP3 markedly enhances AM-evoked internalization of the mutant heterodimers, although there was no change in agonist affinity. Truncating the C-tails by removing the six C-terminal amino acids of hRAMP2 and -3 or exchanging their C-tails with one another had no effect on surface expression, agonist affinity, or internalization of hCRLR, which suggests that the highly conserved Ser-Lys sequence within hRAMP C-tails is involved in cellular trafficking of the two AM receptors. Notably, deleting the respective C-tails from hRAMPs had no effect on lysosomal sorting of hCRLR. Thus, the respective C-tails of hRAMP2 and -3 differentially affect hCRLR surface delivery and internalization.

CGRP[2] and AM belong to the calcitonin family of regulatory molecules and exert a wide variety of biological effects, including potent vasorelaxation (1–3). The receptors that mediate these effects are heterodimers composed of CRLR and RAMP, a novel accessory protein (4). The three RAMP isoforms (RAMP1, RAMP2, and RAMP3) are each composed of ~160 amino acids, and all exhibit a common structure that includes a large extracellular N-terminal domain, a single membrane-spanning domain, and a very short C-tail, but they share less than 30% sequence identity and differ in their tissue distributions (4, 5). When acting as a chaperone, each RAMP forms a 1:1 heterodimer with CRLR, probably in the ER (4, 6). They then mediate the transport of CRLR to the cell surface, where the heterodimers form functional CGRP or AM receptors: CRLR/RAMP1 forms the $CGRP_1$ receptor (4), which can also be activated by high concentrations of AM (7, 8); CRLR/RAMP2 forms an AM-specific receptor that is sensitive to the AM receptor antagonist AM-(22–52) (AM_1 receptor) (7, 9); and CRLR/RAMP3 forms an AM receptor that is sensitive to both the $CGRP_1$ receptor antagonist CGRP-(8–37) and AM-(22–52) (AM_2 receptor) (7, 9). It is the RAMP extracellular domain that mediates agonist binding to CRLR/RAMP heterodimers (11–13), which in turn mediate intracellular cAMP production and Ca^{2+} mobilization (4, 10).

Exposing cells that express GPCRs to their respective agonists frequently leads to a rapid internalization of the receptor in a process believed to involve clathrin-coated vesicles, caveolin-rich vesicles, or both (14, 15). The internalized GPCRs may be recycled back to the plasma membrane in order to promote functional restoration of signal transduction, or they may be trafficked to lysosomes, where they are degraded (14, 15). Similarly, upon binding their respective agonist, hCRLR/RAMP heterodimers stably expressed in HEK-293 cells are rapidly internalized without dissociation via clathrin-coated vesicles (6, 10) in a process that is blocked by dominant negative mutants of dynamin and β-arrestin 2 (6). In that regard, it is well known that G protein-coupled receptor kinases phosphorylate serine/threonine sites located in many GPCR C-tails, enabling β-arrestins to bind there (16). After internalization, both CRLR and RAMP are targeted to lysosomes (10), where they are degraded (6).

Although short, the RAMP C-tails do contain potential sites of interaction with other proteins (5, 17). For instance, the hRAMP3 C-tail possesses a classical type I PDZ (PSD-95/Disc-large/ZO-1) binding motif (TLL) (5, 17), and the binding of NSF to the PDZ motif of hRAMP3 was found to promote slow recycling of internalized hCRLR/hRAMP3 heterodimers in HEK-293 cells (18). In addition, a five-residue motif (QSKRT) in the hRAMP1 C-tail can act as an ER retention signal (19). The C-tails of RAMPs, like that of CRLR, also contain potential phosphorylation and ubiquitination sites (5, 17). Ubiquitination is the post-translational attachment of ubiquitin lysine residues in the substrate proteins (20, 21); it is not crucial for receptor internalization but is essential for proper trafficking to lysosomes for degradation (22, 23). Whether the phosphorylation and ubiquitination sites are also involved

* This work was supported in part by grants-in-aid for scientific research on priority areas and for the 21st Century Centers of Excellence Program (Life Science) from the Ministry of Education, Culture, Sports, Science, and Technology, Japan. The costs of publication of this article were defrayed in part by the payment of page charges. This article must therefore be hereby marked "*advertisement*" in accordance with 18 U.S.C. Section 1734 solely to indicate this fact.

[S] The on-line version of this article (available at http://www.jbc.org) contains one supplemental figure.

[1] To whom correspondence should be addressed. Tel.: 81-985-85-0872; Fax: 81-985-85-6596; E-mail: kuwasako@fc.miyazaki-med.ac.jp.

[2] The abbreviations used are: CGRP, calcitonin gene-related peptide; hαCGRP, human αCGRP; AM, adrenomedullin; hAM, human AM; CRLR, calcitonin receptor-like receptor; hCRLR, human CRLR; RAMP, receptor activity-modifying protein; C-tail, cytoplasmic C-terminal tail; ER, endoplasmic reticulum; GPCRs, G protein-coupled receptors; NSF, *N*-ethylmaleimide-sensitive factor; hNSF, human NSF; PDZ, PSD-95/Disc-large/ZO-1; FITC, fluorescein isothionate; PE, phycoerythrin; HEK, human embryonic kidney; GFP, green fluorescent protein; FACS, fluorescence-activated cell sorting; PBS, phosphate-buffered saline; NHERF, Na^+/H^+ exchanger regulatory factor; β_2-AR, β_2-adrenergic receptor.

in intracellular trafficking of CRLR/RAMP heterodimers remains unknown. To address that issue, we examined the effects of expressing various hRAMP C-tail deletion and progressive truncation mutants and chimeras in which the C-tails were exchanged among the three hRAMPs in HEK-293 cells stably expressing hCRLR.

EXPERIMENTAL PROCEDURES

Materials—^{125}I-[Tyr^0]hαCGRP (specific activity 2 μCi/pmol) (24), which contains an extra N-terminal tyrosine residue (Tyr^0), and ^{125}I-hAM (specific activity 2 μCi/pmol) (1) were both produced in our laboratory. Human αCGRP was purchased from Peptide Institute (Osaka, Japan). [Tyr^0]hαCGRP was from Phoenix Pharmaceuticals, Inc. Human AM was kindly donated by Shionogi & Co. (Osaka, Japan). Mouse anti-hNSF antibody was from Calbiochem. Mouse anti-V5 antibody and FITC-conjugated mouse anti-V5 monoclonal antibody (anti-V5-FITC antibody) were from Invitrogen. Rabbit anti-calnexin antibody was from Stressgen Biotechnologies Corp. (Victoria, Canada), and Alexa Fluor® 594 (biotin- and fluorescent dye-labeled goat anti-rabbit IgG antibody) were from Molecular Probes, Inc. (Eugene, OR). PE-conjugated rabbit anti-mouse secondary antibody was from Exalpha Biologicals, Inc. All other reagents were of analytical grade and were obtained from various commercial suppliers.

Expression Constructs—hNSF (GenBank™ accession number BC030613) was cloned from cDNA obtained from human heart (Clontech) using PCR with the appropriate primers and then modified to provide a consensus Kozak sequence as previously described (25). hRAMP1, -2, and -3 (4) were also modified to provide the same Kozak sequence. A double V5 epitope tag (GKPIPNPLLGLDST) was ligated, in frame, to the 5′-end of the cDNAs encoding each intact hRAMP, and the native signal sequences were removed and replaced with MKTI-LALSTYIFCLVFA (26), yielding V5-hRAMP1, -2, and -3. The deletion and progressive truncation mutations in the V5-hRAMP C-tails were created by using 3′-primers that introduced a translational stop codon at the desired positions (Fig. 1); with RAMP3, for instance, Δ139 represents a mutant in which a stop codon was introduced after residue 139. In addition, various V5-hRAMP chimeras were constructed by exchanging the 9 C-terminal amino acid residues among the three hRAMPs. The hNSF, V5-hRAMPs, V5-hRAMP deletion and truncation mutants, and V5-hRAMP chimeras were then respectively cloned into the mammalian expression vector pCAGGS/Neo (10) using the 5′-XhoI and 3′-NotI sites, and the sequences of the resultant constructs were all verified using an Applied Biosystems 310 Genetic Analyzer. The individual V5-hRAMPs were compared with the native sequence in the assays and were found to behave identically (data not shown).

Cell Culture and DNA Transfection—HEK-293 cells stably expressing a hCRLR-GFP chimera (10) were maintained in Dulbecco's modified Eagle's medium supplemented with 10% fetal bovine serum, 100 units/ml penicillin G, 100 μg/ml streptomycin, 0.25 μg/ml amphotericin B, and 0.25 mg/ml G 418 at 37 °C under a humidified atmosphere of 95% air, 5% CO_2. For experimentation, cells were seeded into 6- or 24-well plates and, upon reaching 70–80% confluence, were transiently cotransfected with the indicated cDNAs using Lipofectamine transfection reagents (Invitrogen) according to the manufacturer's instructions. Briefly, the cells were incubated for 4 h in Opti-MEM I medium containing plasmid DNAs, Plus reagent, and Lipofectamine (see Ref. 27 for 6-well and Ref. 11 for 24-well plates). As a control, some cells were transfected with empty vector (mock). All experiments were carried out 48 h after transfection.

FACS Analysis—Flow cytometry was carried out to assess the levels of cell surface expression of V5-hRAMPs, V5-hRAMP truncation

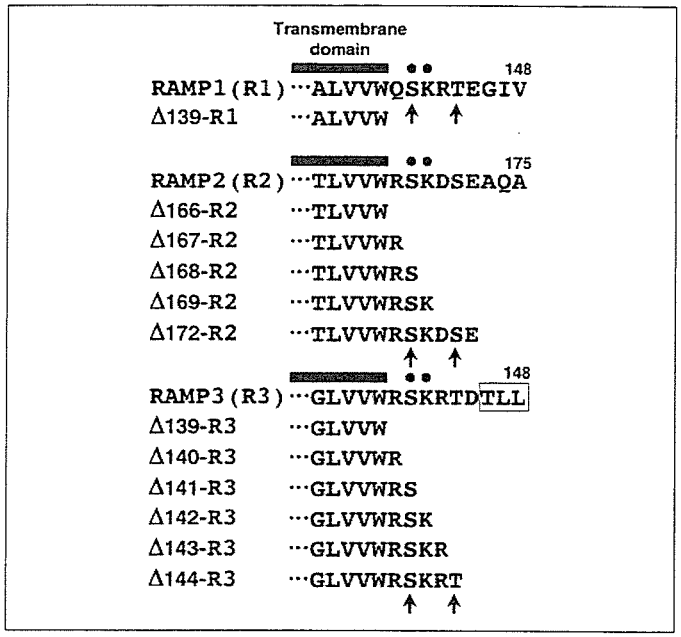

FIGURE 1. **Amino acid sequence alignment of the cytoplasmic tails of hRAMP1, -2, and -3.** The sequences are aligned for maximum homology; alignment of the entire sequences was presented by MacLatchie *et al.* (4). The *numbers* indicate the amino acid positions in accordance with Sexton *et al.* (5). *Black circles* indicate conserved amino acids; *arrows* indicate potential phosphorylation sites; and the PDZ binding motif is *boxed*. The progressive hRAMP C-tail truncation mutants were created using 3′-primers that introduced a translational stop codon at the indicated positions; for instance, Δ139 represents a truncation mutant that introduced a stop codon after residue 139.

mutants, or V5-hRAMP chimeras in HEK-293 cells. To evaluate cell surface expression, cells were harvested following transient transfection, washed twice with PBS, resuspended in ice-cold FACS buffer (27), and then incubated for 60 min at 4 °C in the dark with anti-V5 monoclonal antibody (1:1000 dilution). Following two additional washes with FACS buffer, the cells were incubated for 60 min at 4 °C in the dark with PE-conjugated rabbit anti-mouse secondary antibody (1:400 dilution) in ice-cold FACS buffer. For evaluation of whole cell expression, cells were first permeabilized using IntraPrep™ reagents (Beckman Coulter, Fullerton, CA) according to the manufacturer's instructions and then incubated with anti-V5-FITC antibody (1:500 dilution) for 15 min at room temperature in the dark. Following two successive washes with FACS buffer, both groups of cells were subjected to flow cytometry in an EPICS XL flow cytometer (Beckman Coulter) and analyzed using EXPO 2 software (Beckman Coulter). Fluorophores were excited at 488 nm, and the emission was monitored at 530 nm for GFP and 575 nm for PE. Viability was assessed by exclusion of propidium iodide.

Immunofluorescence Microscopy—HEK-293 cells stably expressing hCRLR-GFP were plated onto 35-mm glass-bottomed dishes (Iwaki, Tokyo, Japan). As determined by the experimental protocol, some cells were then transiently transfected with V5-hRAMP2, Δ166-hRAMP2, or Δ167-hRAMP2. The cells were then fixed with 3.7% formaldehyde in PBS for 20 min at room temperature, washed twice with PBS, and permeabilized with 0.25% Triton X-100 in PBS for 10 min. Thereafter, the cells were incubated at room temperature for 30 min in blocking buffer (PBS containing 1% bovine serum albumin), followed by incubation for 60 min first with rabbit anti-calnexin (1:200 dilution) and mouse anti-V5-FITC antibody (1:500 dilution) and then, after washing four times with PBS, with the Alexa Fluor® 594 diluted 1:100 in blocking buffer. After another three washes with PBS, the cells were mounted using Slow-Fade mounting medium (Molecular Probes, Inc.), and a 22-mm glass coverslip was seated in the center of each dish. Double labeling was

viewed using a TCS-SP2 AOBS confocal laser-scanning microscope (Leica) equipped with a × 63/1.32 numerical aperture immersion lens (Leica).

Whole-cell Radioligand Binding Assays—Transfected HEK-293 cells in 24-well plates were washed twice with prewarmed PBS and then incubated for 5 h at 4 °C with ^{125}I-[Tyr^0]hαCGRP (100 pM) or ^{125}I-hAM (20 pM) in the presence (for nonspecific binding) or absence (for total binding) of 1 μM unlabeled hαCGRP or hAM in modified Krebs-Ringer-HEPES medium (10), after which they were washed twice more with ice-cold PBS and harvested with 0.5 M NaOH. The associated cellular radioactivity was measured in a γ-counter. Specific binding was defined as the difference between total binding and nonspecific binding.

cAMP Measurements—Transfectants in 24-well plates were incubated for 15 min at 37 °C in Hanks' buffer containing 20 mM HEPES, 0.2% bovine serum albumin, 0.5 mM 3-isobutyl-1-methylxanthine (Sigma), and the indicated concentrations of hαCGRP or hAM. The reaction mixture was then replaced with 20 mM HCl and 1 M acetic acid to extract the intracellular cAMP, after which the resultant extracts were lyophilized and stored at −30 °C until assayed. The cAMP concentrations were measured using our specific radioimmunoassay (1).

FACS Analysis of Receptor Internalization and Recycling—Following cotransfection of the indicated cDNAs into HEK-293 cells stably expressing hCRLR-GFP in 6-well plates, the cells were exposed to selected concentrations of hαCGRP or hAM in prewarmed serum-free Dulbecco's modified Eagle's medium containing 20 mM HEPES and 0.2% bovine serum albumin for the indicated periods (up to 2 h) at 37 °C. For receptor recycling studies, the cells were incubating for 60 min with the agonist plus 10 μg/ml cycloheximide and 10 μg/ml brefeldin A and then washed three times with prewarmed PBS. The medium was then replaced with prewarmed Dulbecco's modified Eagle's medium containing 20 mM HEPES, 10% fetal bovine serum, 10 μg/ml cycloheximide, and 10 μg/ml brefeldin A for the indicated periods (up to 4 h) at 37 °C. Internalization and recycling were stopped by adding ice-cold PBS, after which the cells were harvested, resuspended in ice-cold FACS buffer, and labeled with anti-V5 monoclonal antibody and fluorescein PE-conjugated rabbit anti-mouse secondary antibody. The cells were then subjected to flow cytometry and analyzed as described above.

mRNA Expression Measured by Real Time Quantitative PCR—Total RNAs were extracted from HEK-293 cells either untransfected or transfected as indicated using total RNA isolation reagent (Invitrogen). Thereafter, the target cDNAs were synthesized from the respective mRNAs by reverse transcription using SuperScript reverse transcriptase (Invitrogen). The expression of mRNAs encoding hNSF was assessed using real time quantitative PCR (Prism 7700 Sequence Detector, Applied Biosystems, Foster City, CA) with original oligonucleotide primers (sense, 5′-AGAACAGTGACCGCACACCAT-3′; antisense, 5′-TCCACAACCACACAACTGAGC-3′) and a fluorescently labeled probe (5′-AGCGTGCTTCTGGAAGGCCCTCCTCACAGT-3′). The size of the amplified DNA was 223 bp. The levels of hNSF mRNA were normalized to those of glyceraldehyde-3-phosphate dehydrogenase mRNA, which served as an internal control.

Western Analysis—Following transient transfection of hNSF into cells plated in 6-well plates, the transfectants were washed twice with ice-cold PBS, harvested in 1 ml of sample buffer (28), and boiled for 10 min. Equal aliquots of protein (20 μg) were then subjected to 10% SDS gel electrophoresis and transferred to a Hybond-P membrane (Amersham Biosciences). The membrane was then blocked with 5% block reagent (Amersham Biosciences), washed, and incubated first for 1 h at room temperature with rabbit anti-hNSF antibody (1:1,000 dilution) and then with secondary antibody (1:10,000 dilution). hNSF proteins were detected using an ECL Plus chemiluminescence kit (Amersham Biosciences), after which they were quantitated by densitometry using Image Gauge (LAS-1000; Fujifilm).

Statistical Analysis—Results are expressed as means ± S.E. of at least three independent experiments. Differences between two groups were evaluated using Student's *t* tests; differences among multiple groups were evaluated with a one-way analysis of variance followed by Scheffe's tests. Values of $p < 0.05$ were considered significant.

RESULTS

Deletion of hRAMP C-tails—We previously established HEK-293 cells stably expressing hCRLR-GFP alone or together with Myc-hRAMPs and used them to visualize the cellular localization and trafficking of hCRLR (10). Following AM exposure, hCRLR is rapidly internalized together with its associated hRAMP, and then both are trafficked to lysosomes; fusion of GFP to the C terminus of hCRLR had no apparent effect on the trafficking of the heterodimeric receptor. In the present study, therefore, we used HEK-293 cells stably expressing hCRLR-GFP to examine the functions of the C-tails of the three hRAMPs within the respective CRLR/RAMP heterodimers.

We initially tested the effect of completely deleting the C-tails of the three V5-epitope tagged hRAMPs (Fig. 2). When coexpressed with hCRLR, V5-RAMP1, -2, and -3 were detected at the surfaces of 45.9, 21.9, and 38.9% of cells, respectively. On the other hand, the V5-RAMP deletion mutants Δ139-RAMP1, Δ166-RAMP2, and Δ139-RAMP3 appeared at the surface of 43.7, 5.0, and 38.8% of cells, respectively. Thus, deletion of the C-tail significantly reduced surface delivery of only RAMP2. Surface immunoreactivity was detected in only 0.55% of cells expressing the empty vector (Mock), which is well within the 2% limit of resolution characteristic of FACS analysis.

We next evaluated the binding profiles of ^{125}I-[Tyr^0]hαCGRP and ^{125}I-hAM to cells expressing each of the wild-type and mutant receptors (Fig. 3, *A* and *B*). When CRLR-GFP was coexpressed with empty vector (*Mock*), the cells showed only very low levels of specific binding of ^{125}I-[Tyr^0]αCGRP and ^{125}I-AM. Co-transfection of RAMP1 led to markedly higher specific ^{125}I-[Tyr^0]αCGRP binding than was seen with Δ139-RAMP1 (Fig. 3*A*), although there was no difference in the surface expression of either heterodimeric receptor (Fig. 2). Likewise, cotransfection of RAMP2 significantly increased the specific binding of

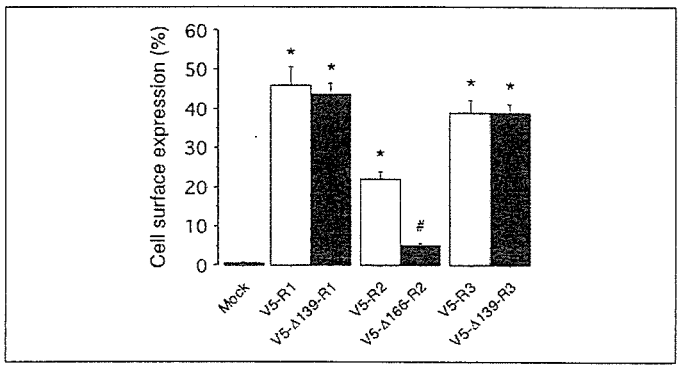

FIGURE 2. **FACS analysis of HEK-293 cells coexpressing hCRLR with intact hRAMP or a C-terminal deletion mutant.** HEK-293 cells stably expressing CRLR-GFP were transiently transfected with empty vector (*Mock*) or the indicated V5-RAMP or deletion mutant. The cells were incubated first with an anti-V5 monoclonal antibody and then with a fluorescein PE-conjugated rabbit anti-mouse secondary antibody. Samples incubated with only secondary antibody served as the control. Cell surface expression of each construct was estimated by flow cytometry. The *bars* represent means ± S.E. of six independent experiments. *, $p < 0.001$ *versus* control (*Mock*); #, $p < 0.02$ *versus* corresponding wild-type V5-RAMP.